

Li depletion in solar analogues with exoplanets

Extending the sample^{*,**}

E. Delgado Mena¹, G. Israelian^{2,3}, J. I. González Hernández^{2,3}, S. G. Sousa^{1,2,4}, A. Mortier^{1,4}, N. C. Santos^{1,4},
V. Zh. Adibekyan¹, J. Fernandes⁵, R. Rebolo^{2,3,6}, S. Udry⁷, and M. Mayor⁷

¹ Centro de Astrofísica, Universidade do Porto, Rua das Estrelas, 4150-762 Porto, Portugal
e-mail: Elisa.Delgado@astro.up.pt

² Instituto de Astrofísica de Canarias, C/ Via Lactea s/n, 38200 La Laguna, Tenerife, Spain

³ Departamento de Astrofísica, Universidad de La Laguna, 38205 La Laguna, Tenerife, Spain

⁴ Departamento de Física e Astronomia, Faculdade de Ciências, Universidade do Porto, 4169-007 Porto, Portugal

⁵ CGUC, Department of Mathematics and Astronomical Observatory, University of Coimbra, 3049 Coimbra, Portugal

⁶ Consejo Superior de Investigaciones Científicas, CSIC, Spain

⁷ Observatoire de Genève, Université de Genève, 51 ch. des Maillettes, 1290 Sauverny, Switzerland

Received 18 March 2013 / Accepted 25 November 2013

ABSTRACT

Aims. We want to study the effects of the formation of planets and planetary systems on the atmospheric Li abundance of planet host stars.

Methods. In this work we present new determinations of lithium abundances for 326 main sequence stars with and without planets in the T_{eff} range 5600–5900 K. The 277 stars come from the HARPS sample, the remaining targets were observed with a variety of high-resolution spectrographs.

Results. We confirm significant differences in the Li distribution of solar twins ($T_{\text{eff}} = T_{\odot} \pm 80$ K, $\log g = \log g_{\odot} \pm 0.2$ and $[\text{Fe}/\text{H}] = [\text{Fe}/\text{H}]_{\odot} \pm 0.2$): the full sample of planet host stars (22) shows Li average values lower than “single” stars with no detected planets (60). If we focus on subsamples with narrower ranges in metallicity and age, we observe indications of a similar result though it is not so clear for some of the subsamples. Furthermore, we compare the observed spectra of several couples of stars with very similar parameters that show differences in Li abundances up to 1.6 dex. Therefore we show that neither age, mass, nor metallicity of a parent star is the only cause for enhanced Li depletion in solar analogues.

Conclusions. We conclude that another variable must account for that difference and suggest that this could be the presence of planets that causes additional rotationally induced mixing in the external layers of planet host stars. Moreover, we find indications that the amount of depletion of Li in planet-host solar-type stars is higher when the planets are more massive than Jupiter.

Key words. stars: abundances – stars: fundamental parameters – planetary systems – planets and satellites: formation – stars: evolution

1. Introduction

The study of extrasolar planets has been an exciting field of astrophysics for more than 15 years. More than 1000 planets are known in almost 800 planetary systems (Encyclopaedia of Extrasolar Planets, Schneider et al. 2011). Photospheric abundances of planet host stars are key to understanding the role of the metallicity of protoplanetary clouds in the formation of planets and to determining how the formation of planets may affect the structure and evolution of the parent stars.

Many studies (e.g. Gonzalez 1997; Santos et al. 2004, 2005; Fischer & Valenti 2005; Sousa et al. 2008) have shown the significant metallicity excess of the planet-host sample compared with the sample of stars without known giant planets, suggesting a possible clue to a formation scenario. However, this metallicity excess does not seem to appear in stars which only host Neptunians and Earth-like planets (Udry & Santos 2007; Sousa et al. 2008, 2011b). These stars have metallicities lower on average than in stars with Jupiters, and more similar to the $[\text{Fe}/\text{H}]$ distribution of stars without detected planets. Interestingly, Adibekyan et al. (2012a,b) have recently shown that even low-mass planet hosts with $[\text{Fe}/\text{H}] < -0.2$ present enhanced abundances of α elements and suggested that a minimum quantity of refractory material is required to form planets when the amount of Fe is low.

King et al. (1997) reported a difference in the Li abundances between the components of the binary 16 Cyg, suggesting that the presence of a planet might be responsible for the lower Li found in its host star. Using a larger sample of stars in the T_{eff} range 5600–5850 K with detected planets, Gonzalez & Laws (2000) and Israelian et al. (2004) show that

* Based on observations collected at the La Silla Observatory, ESO (Chile), with the HARPS spectrograph at the 3.6 m ESO telescope, with CORALIE spectrograph at the 1.2 m Euler Swiss telescope and with the FEROS spectrograph at the 1.52 m ESO telescope; at the Paranal Observatory, ESO (Chile), using the UVES spectrograph at the VLT/UT2 Kueyen telescope, and with the FIES, SARG, and UES spectrographs at the 2.5 m NOT, the 3.6 m TNG and the 4.2 WHT, respectively, operated on the island of La Palma in the Spanish Observatorio del Roque de los Muchachos.

** Table 6 is available in electronic form at <http://www.aanda.org>

exoplanets hosts are significantly more Li-depleted than stars without detected planets (hereafter called single stars¹). This result was also supported by [Takeda & Kawanamoto \(2005\)](#), [Chen & Zhao \(2006\)](#), and [Gonzalez \(2008\)](#). [Israelian et al. \(2009\)](#) confirm former results using the homogeneous and high-quality HARPS GTO sample. They find that about 50% of 60 solar analogues ($T_{\text{eff}} = T_{\odot} \pm 80$ K) without detected planets had $A(\text{Li}) \geq 1.5$, while only 2 out of 24 planet hosts had high Li abundances. Other recent works by [Takeda et al. \(2010\)](#) and [Gonzalez et al. \(2010\)](#) have also reported similar results. Furthermore, [Sousa et al. \(2010\)](#) show that mass and age are not responsible for the observed correlation using the same sample as in [Israelian et al. \(2009\)](#). Doubts about the proposed Li-planet connection have been raised in several works ([Ryan 2000](#); [Luck & Heiter 2006](#); [Baumann et al. 2010](#); [Ghezzi et al. 2010](#); [Ramírez et al. 2012](#)) and argue that the observed behaviour of Li abundances could be associated to age, mass, or metallicity differences between stars with and without planets. However, this cannot be the ultimate explanation of the observed behaviour of Li in planet host stars, since several old stellar clusters like M 67 have shown that solar-type stars of very similar age and metallicity present a wide dispersion of Li abundances ([Randich et al. 2007](#); [Pasquini et al. 2008](#); [Pace et al. 2012](#)). What is then the principal parameter that accounts for this scatter in Li abundances?

Lithium is formed in a significant quantity at the primordial nucleosynthesis and is easily destroyed by (p, α)-reactions at 2.5 million K in the inner layers of solar-type stars. Although Li depletion occurs primarily in the pre-main sequence (PMS), it can also take place in stellar envelopes if any extra mixing process exists. In fact, there is an obvious relation between T_{eff} and Li-depletion: cooler stars are more Li-depleted because of their thicker convective envelopes (where Li is brought to hotter layers to be depleted).

It seems that rotation-induced mixing and angular momentum loss are the most efficient processes destroying Li in solar-type stars on the main sequence (MS; e.g. [Zahn 1992](#); [Pinsonneault et al. 1992](#); [Deliyannis & Pinsonneault 1997](#)). Observations indicate that rapidly rotating stars preserve more Li than slow rotators of the same mass, as observed in Pleiades ([Soderblom et al. 1993](#); [Garcia Lopez et al. 1994](#)) or IC 2602 ([Randich et al. 1997](#)). This is also found in solar-type stars by [Takeda et al. \(2010\)](#) and [Gonzalez et al. \(2010\)](#). Other invoked mechanisms are internal waves (e.g. [Montalbán & Schatzman 1996](#)) or overshooting mixing, recently claimed as being a primary depletion mechanism (e.g. [Xiong & Deng 2009](#); [Zhang 2012](#)). Some works have also combined several mechanisms showing that the efficiency of rotational mixing is decreased when magnetic fields are taken into account ([Eggenberger et al. 2010](#)), as well as when there are internal gravity waves ([Charbonnel & Talon 2005](#)) since they lead to efficient angular momentum redistribution from the core to the envelope.

Other mechanisms directly related to the presence of planets have been proposed as causing additional Li depletion. For instance, [Israelian et al. \(2004\)](#), [Chen & Zhao \(2006\)](#), and [Castro et al. \(2009\)](#) have suggested that Li depletion could be related to planet migration since it can create a shear instability that produces effective mixing. It is also possible that proto-planetary discs lock a large amount of angular momentum and therefore create some rotational breaking in the host stars during the

PMS inducing an increased mixing ([Israelian et al. 2004](#)). This possibility has also been proposed by [Bouvier \(2008\)](#) using simple rotational models: long-lived accretion discs of stars with low initial velocities lead to the formation of a large velocity shear in the base of the convective zone. The velocity gradient in turn triggers hydrodynamical instabilities responsible for enhanced lithium burning on PMS and MS evolution scales. This explanation matches the Li depletion in planet hosts well since we expect long disc lifetimes in order to form planets. The relation of long-lived discs with slow rotation on the ZAMS has also been probed by [Eggenberger et al. \(2012\)](#) as well as the increase of rotational mixing (and thus Li depletion) when differential rotation rises in the stellar interior during PMS. Finally, the infall of planetary material might also affect the mixing processes of those stars by thermohaline convection ([Garaud 2011](#); [Théado & Vauclair 2012](#)), as well as the episodic accretion of planetary material can increase the temperature in the bottom of the convective envelope, hence increase Li depletion ([Baraffe & Chabrier 2010](#)).

The above mentioned theoretical studies and models propose a clear relationship among stellar rotation (PMS or MS), formation and evolution of planets, and surface Li abundances of solar type stars. To discover this relation observationally, homogeneous and precise studies of planet host stars have to be undertaken. In this paper we extend our previous Li work ([Israelian et al. 2009](#)) by including new stars observed in HARPS surveys and at other telescopes.

2. Observations and stellar samples

The principal sample used in this work is formed by 1111 FGK stars observed within the context of the HARPS GTO programmes to search for planets. The stars in that project were selected from a volume-limited stellar sample observed by the CORALIE spectrograph at La Silla observatory ([Udry et al. 2000](#)). The stars were selected to be suitable for radial velocity surveys. They are slow rotating and non-evolved solar type dwarfs with spectral type between F2 and M0 that also do not show a high level of chromospheric activity. The final sample is a combination of three HARPS subsamples hereafter called HARPS-1 ([Mayor et al. 2003](#)), HARPS-2 ([Lo Curto et al. 2010](#)) and HARPS-4 ([Santos et al. 2011](#)). Note that the HARPS-2 planet search programme is the complementation of the previously started CORALIE survey ([Udry et al. 2000](#)) to fainter magnitudes and to a larger volume.

The individual spectra of each star were reduced using the HARPS pipeline and then combined with IRAF³ after correcting for its radial velocity. The final spectra have a resolution of $R \sim 115\,000$ and high signal-to-noise ratio (55% of the spectra have S/N higher than 200), depending on the amount and quality of the original spectra. The total sample is composed of 135 stars with planets and 976 stars without detected planets, but in our effective temperature region of interest (5600–5900 K) we have 42 and 235 stars with and without planets. To increase the number of stars with planets we used spectroscopic data for 49 planet hosts which come from different observing runs, listed in Table 1, some of them belonging to the CORALIE survey (see Table 4). The data reduction was made with the IRAF package or with the respective telescopes pipelines. All the images were flat-field-corrected, sky-subtracted, and added

¹ We adopt this term for the sake of simplicity throughout the paper. We warn the reader not to confuse it with the term typically given to non-binary stars.

² $T_{\odot} = 5777$ K.

³ IRAF is distributed by National Optical Astronomy Observatories, operated by the Association of Universities for Research in Astronomy, Inc., under contract with the National Science Foundation, USA.

Table 1. Observing details: telescopes, spectrographs, resolving power, and spectral ranges used in this work.

Telescope	Instrument	Resolution $\lambda/\delta\lambda$	Spectral range Å
3.6-m ESO La Silla Observatory (Chile)	HARPS	100 000	3.800–7.000
8.2-m Kueyen UT2 (VLT)	UVES	115 000	3.000–4.800, 4.800–6.800
2.2-m ESO/MPI telescope	FEROS	48 000	3.600–9.200
3.5-m TNG	SARG	57 000/86 000	5.100–10.100
2.6-m Nordic Optical Telescope	FIES	67 000	3.700–7.300
1.93-m OHP	SOPHIE	75 000	3.820–6.930
1.2-m Euler Swiss telescope	CORALIE	50 000	3.800–6.800
4.2-m <i>William Herschel</i> Telescope	UES	55 000	4.600–7.800

Table 2. Definition of the subsamples in this work.

Name	T_{eff} (K)	[Fe/H]	$\log g$ (cm s^{-2})	Planet hosts ^a	Single stars	Planet hosts $A(\text{Li}) > 1.4$	Single stars $A(\text{Li}) > 1.4$
Solar type	5600, 5900	−0.85, 0.5	3.8, 4.7	43+49	233 ^b	28% +5% −4%	43% ± 3%
Solar analogues	5697, 5857	−0.6, 0.5	4.24, 4.64	18+25	99	19% +7% −4%	47% ± 5%
Solar twins	5697, 5857	−0.2, 0.2	4.24, 4.64	9+13	60	18% +10% −5%	48% ± 6%

Notes. ^(a) Planets hosts from HARPS (including the Sun)+planet hosts from other surveys. ^(b) There are 2 more stars in this T_{eff} range with metallicities −1.04 and −1.07 shown in Table 6.

to obtain 1D spectra. Doppler correction was also done. We note that our sample contains 98% of planets hosts within the range 5600–5900 K discovered by radial velocities and 77% if we also consider the transiting planet hosts (Santos et al. 2013).

3. Analysis

The stellar atmospheric parameters were taken from Sousa et al. (2008, 2011a,b) for HARPS stars and from Santos et al. (2004, 2005), Sousa et al. (2006) and Mortier et al. (2013) for the rest of the planet hosts. The errors of the parameters from Santos et al. (2004, 2005) are of the order of 44 K for T_{eff} , 0.11 dex for $\log g$, 0.08 km s^{-1} for ξ_t , 0.06 dex for metallicity and 0.05 M_{\odot} for the masses. From Sousa et al. (2008, 2011a,b), the typical errors are 30 K for T_{eff} , 0.06 dex for $\log g$, 0.08 km s^{-1} for ξ_t , and 0.03 dex for metallicity. We refer to those works for further details in the parameters determination and errors. All the sets of parameters were determined in a consistent way so as to reduce at maximum the systematic errors. We note here the uniformity of the adopted stellar parameters as discussed in Sect. 5 of Sousa et al. (2008). Our group is continuously updating the stellar parameters of stars under consideration (Sousa et al. 2008, 2011a,b) and has created an online catalogue (Santos et al. 2013) to guarantee a homogeneous and precise study of stellar abundances. This is especially important for Li when we have clearly limited the study to solar analogues.

Li abundances, $A(\text{Li})^4$, were derived by standard LTE analysis using spectral synthesis with the revised version of the spectral synthesis code MOOG2010 (Snedden 1973) and a grid of Kurucz ATLAS9 atmospheres with overshooting (Kurucz 1993). We used the linelist from Ghezzi et al. (2009) though we applied a slight correction to the $\log gf$ (to −2.278) of Fe I line at 6707.4 Å to adjust the Kurucz Solar Flux Atlas spectrum (Kurucz et al. 1984). We neglected possible ⁶Li contributions. We did not apply NLTE corrections since for this kind of star they are quantitatively insignificant compared to the large dispersion of Li abundances or to a conservative typical error of 0.1 dex (Takeda & Kawonomoto 2005; Ramírez et al. 2012).

Some examples of spectral synthesis are shown in Fig. 1. All abundances and their errors are listed in Tables 3, 4, and 6⁵.

Stellar masses and ages were derived by using the stellar evolutionary models from the Padova group computed with the web interface⁶ dealing with stellar isochrones and their derivatives to the stars of our sample. The values for T_{eff} and [Fe/H] were taken from the previously mentioned works and V magnitudes and parallaxes come from the Hipparcos database. For those stars with no values in Hipparcos database we used other sources as Simbad database⁷ or The Extrasolar Planets Encyclopaedia⁸ (Schneider et al. 2011).

4. Discussion

In Fig. 2 we present a general overview of the behaviour of Li as a function of effective temperature for solar type stars. We can see in the plot the ranges in T_{eff} , [Fe/H] and gravity for the stars in this sample (see also Table 2). As expected, below 5650 K, most of the stars have severe depleted Li abundances regardless of whether they have planets or not. These stars have deeper convective envelopes that allow the material to reach the Li-burning layers on the MS. However, a similar depletion of Li is also observed in stars with slightly higher temperatures (around solar T_{eff}). Standard models (Deliyannis et al. 1990; Pinsonneault 1997), which only consider mixing by convection, do not predict the Li depletion observed in solar-type stars. Indeed, the location of the base of the solar convection zone inferred from helioseismology is not hot enough to burn Li on the MS (Christensen-Dalsgaard et al. 1991).

On the other hand, when the temperature is close to 5900 K, most of the stars have preserved higher amounts of Li (due to their shallower convective envelopes) but still present signs of depletion that are not expected from canonical models either (e.g. Pinsonneault 1997). Therefore, there must be other

⁵ We note that there are some stars in common between the three used HARPS samples. We only used the best available spectrum for each of those, with its corresponding parameters as shown in these tables.

⁶ <http://stev.oapd.inaf.it/cgi-bin/param>

⁷ <http://simbad.u-strasbg.fr/simbad/sim-fid>

⁸ <http://exoplanet.eu/catalog/>

⁴ $A(\text{Li}) = \log[N(\text{Li})/N(\text{H})] + 12$.

Table 3. Li abundances for stars with planets from HARPS GTO samples.

Star	T_{eff} (K)	$\log g$ (cm s^{-2})	ξ_t (km s^{-1})	[Fe/H]	Age (Gyr)	Mass (M_{\odot})	A(Li)	Error	$M \sin i$ (M_J)
HARPS-1									
HD 1461 ^a	5765	4.38	0.97	0.19	3.73	1.05	0.68	0.10	0.024
HD 4308 ^a	5644	4.38	0.90	-0.34	11.72	0.82	0.96	0.06	0.041
HD 16141	5806	4.19	1.11	0.16	6.55	1.07	1.25	0.10	0.215
HD 16417 ^a	5841	4.16	1.18	0.13	5.99	1.12	1.80	0.04	0.069
HD 20782	5774	4.37	1.00	-0.06	9.21	0.94	<0.47	-	1.900
HD 28185	5667	4.42	0.94	0.21	3.38	1.02	<0.26	-	5.700
HD 31527 ^a	5898	4.45	1.09	-0.17	7.57	0.95	1.91	0.03	0.052
HD 38858 ^a	5733	4.51	0.94	-0.22	8.48	0.89	1.49	0.05	0.096
HD 45184 ^a	5869	4.47	1.03	0.04	2.28	1.05	2.06	0.04	0.040
HD 47186	5675	4.36	0.93	0.23	4.57	1.02	0.58	0.10	0.351
HD 65216	5612	4.44	0.78	-0.17	6.20	0.89	1.23	0.05	1.210
HD 66428	5705	4.31	0.96	0.25	5.26	1.03	<0.71	-	2.820
HD 70642	5668	4.40	0.82	0.18	2.69	1.02	<0.46	-	2.000
HD 92788	5744	4.39	0.95	0.27	1.81	1.05	0.62	0.07	3.860
HD 96700 ^a	5845	4.39	1.04	-0.18	10.53	0.93	1.27	0.08	0.040
HD 102117	5657	4.31	0.99	0.28	8.40	1.01	0.52	0.10	0.172
HD 102365 ^a	5629	4.44	0.91	-0.29	11.32	0.85	<0.30	-	0.050
HD 107148	5805	4.40	0.93	0.31	3.63	1.07	<1.34	-	0.210
HD 114729	5844	4.19	1.23	-0.28	11.00	0.95	1.95	0.04	0.840
HD 117207	5667	4.32	1.01	0.22	6.31	1.01	<0.12	-	2.060
HD 134987	5740	4.30	1.08	0.25	6.29	1.04	<0.60	-	1.590
HD 141937	5893	4.45	1.00	0.13	1.08	1.09	2.35	0.04	9.700
HD 147513	5858	4.50	1.03	0.03	0.64	1.05	2.05	0.05	1.210
HD 160691	5780	4.27	1.09	0.30	6.36	1.07	0.98	0.10	1.814
HD 190647	5639	4.18	0.99	0.23	8.47	1.04	<0.51	-	1.900
HD 202206	5757	4.47	1.01	0.29	1.97	1.06	1.37	0.05	17.400
HD 204313	5776	4.38	1.00	0.18	3.03	1.05	<0.52	-	3.550
HD 222582	5779	4.37	1.00	-0.01	7.48	0.97	0.85	0.15	7.750
HD 126525	5638	4.37	0.90	-0.10	9.60	0.89	<-0.01	-	0.224
HD 134606	5633	4.38	1.00	0.27	7.09	0.99	<0.39	-	0.121
HD 136352 ^a	5664	4.39	0.90	-0.34	11.73	0.84	<-0.10	-	0.036
HD 150433	5665	4.43	0.88	-0.36	11.43	0.82	<0.27	-	0.168
HD 189567 ^a	5726	4.41	0.95	-0.24	11.55	0.87	<0.18	-	0.032
HD 215456	5789	4.10	1.19	-0.09	8.37	1.05	2.31	0.04	0.246
HARPS-4									
HD 171028	5671	3.84	1.24	-0.48	-	-	<0.04	-	1.980
HD 181720	5792	4.25	1.16	-0.53	11.22	0.92	1.93	0.02	0.370
HARPS-2									
HD 6718	5723	4.44	0.84	-0.07	6.54	0.95	<0.47	-	1.560
HD 28254	5653	4.15	1.08	0.36	7.75	1.06	<0.59	-	1.160
HD 30177	5601	4.34	0.89	0.37	5.66	0.99	<0.51	-	7.700
HD 44219	5766	4.20	1.06	0.04	8.43	1.01	1.23	0.10	0.580
HD 109271 ^a	5783	4.28	0.97	0.10	7.30	1.05	1.42	0.08	0.076
HD 207832	5718	4.45	0.86	0.15	1.90	1.01	<1.04	-	0.730

Notes. Parameters from [Sousa et al. \(2008, 2011a,b\)](#). The minimum mass of the most massive planet in the system is indicated in the last column (taken from The Extrasolar Planets Encyclopaedia, [Schneider et al. 2011](#)). ^(a) Stars which only host Neptune and Earth-like planets.

mechanisms such as rotationally induced mixing ([Pinsonneault et al. 1990](#)), diffusion ([Richer & Michaud 1993](#)), internal waves ([Montalbán & Schatzman 2000](#)), overshooting (e.g. [Xiong & Deng 2009](#)) or the combination of several (e.g. [Chaboyer et al. 1995](#); [Charbonnel & Talon 2005](#)), that account for the destruction of Li observed in solar-type stars in open clusters and in the field (e.g. [Pace et al. 2012](#)).

As seen in Fig. 2, there is a high dispersion in Li abundances in the T_{eff} interval 5600–5900 K. Most of the planet hosts have destroyed their Li in this T_{eff} window. To better appreciate the effects of planets on Li depletion we now focus in the solar temperature range, $T_{\text{eff}} = T_{\odot} \pm 80$ K, where previous works found differences between both groups of stars

(e.g. [Israelian et al. 2009](#)). In this range of temperatures the convective envelope is not as deep as in cooler stars but lies very close to the Li burning layer. If some mechanism exists that is capable of producing an extra mixing (even if it is not very intense), Li will therefore suffer some depletion. As a consequence, this type of stars is very sensitive to non-standard mixing processes.

Below we discuss the dependence of Li depletion on several parameters. It is important to note that to make a meaningful comparison of planet hosts and single stars, we have to deal with solar-type stars in the MS. Therefore, we removed from our sample of planet hosts some stars showing activity and/or with very young ages such as HD 81040, which has a disc ([Sozzetti et al. 2006](#)); HD 70573 ([Setiawan et al. 2007](#)); or

Table 4. Planet hosts stars not belonging to the HARPS-GTO sample.

Star	T_{eff} (K)	$\log g$ (cm s^{-2})	ξ_t (km s^{-1})	[Fe/H]	Age (Gyr)	Mass (M_{\odot})	A(Li)	Error	$M \sin i$ (M_J)	Flag	Reference
HD 45350	5650	4.29	1.08	0.28	8.22	1.01	<0.52	–	1.790	[6]	this work
HD 79498	5814	4.40	1.09	0.24	1.10	1.08	1.28	0.10	1.340	[6]	this work
HD 179079 ^a	5742	4.11	1.22	0.26	6.86	1.09	2.01	0.05	0.080	[6]	this work
HIP 14810	5601	4.43	0.96	0.26	4.35	0.99	<0.84	–	3.880	[1]	this work
HD 4113	5688	4.40	1.08	0.20	5.39	1.01	<0.86	–	1.560	[5]	Tamuz et al. (2008)
HD 4203	5636	4.23	1.12	0.40	8.23	1.01	<0.65	–	2.070	[3]	Santos et al. (2004)
HD 6434	5835	4.60	1.53	–0.52	10.21	0.86	<0.79	–	0.390	[3]	Santos et al. (2004)
HD 12661	5702	4.33	1.05	0.36	5.84	1.02	<0.63	–	2.300	[8]	Santos et al. (2004)
HD 49674	5644	4.37	0.89	0.33	2.13	1.01	<1.00	–	0.115	[4]	Santos et al. (2004)
HD 73526	5699	4.27	1.26	0.27	7.28	1.05	0.63	0.10	2.900	[1]	Santos et al. (2004)
HD 76700	5737	4.25	1.18	0.41	6.80	1.05	1.27	0.10	0.190	[1]	Santos et al. (2004)
HD 106252	5899	4.34	1.08	–0.01	3.52	1.03	1.71	0.05	7.560	[1]	Santos et al. (2004)
HD 109749	5899	4.31	1.13	0.32	2.98	1.12	2.24	0.05	0.280	[5]	Sousa et al. (2006)
HD 114762	5884	4.22	1.31	–0.70	11.61	0.87	2.07	0.03	10.980	[1]	Santos et al. (2004)
HD 154857	5610	4.02	1.30	–0.23	4.52	1.22	1.68	0.03	1.800	[3]	Santos et al. (2005)
HD 168443	5617	4.22	1.21	0.06	9.68	1.01	<0.45	–	17.193	[4]	Santos et al. (2004)
HD 178911B	5600	4.44	0.95	0.27	5.38	0.99	<0.94	–	6.292	[4]	Santos et al. (2004)
HD 186427	5772	4.40	1.07	0.08	6.23	1.00	<0.52	–	1.680	[4]	Santos et al. (2004)
HD 187123	5845	4.42	1.10	0.13	4.53	1.05	<0.54	–	1.990	[4]	Santos et al. (2004)
HD 188015	5793	4.49	1.14	0.30	2.22	1.07	<0.87	–	1.260	[3]	Santos et al. (2005)
HD 195019	5859	4.32	1.27	0.09	6.53	1.07	1.53	0.06	3.700	[8]	Santos et al. (2004)
HD 216437	5887	4.30	1.31	0.25	4.65	1.15	1.99	0.06	1.820	[1]	Santos et al. (2004)
HD 217014	5804	4.42	1.20	0.20	3.94	1.06	1.29	0.10	0.468	[3]	Santos et al. (2004)
HD 217107	5645	4.31	1.06	0.37	7.30	0.99	<0.61	–	2.490	[3]	Santos et al. (2004)
HD 9446	5793	4.53	1.01	0.09	2.49	1.03	1.82	0.05	1.820	[7]	Hébrard et al. (2010)
HD 109246	5844	4.46	1.01	0.10	2.08	1.04	1.58	0.10	0.770	[7]	Boisse et al. (2010)
Kepler-17	5781	4.53	1.73	0.26	3.68	1.07	<1.38	–	2.450	[7]	Bonomo et al. (2012)
KOI-204	5757	4.15	1.75	0.26	4.03	1.06	<1.38	–	1.020	[7]	Bonomo et al. (2012)
XO-1	5754	4.61	1.07	–0.01	–	–	1.33	0.12	0.900	[4]	Ammler-von Eiff et al. (2009)
HD 23127	5891	4.23	1.26	0.41	4.32	1.20	2.67	0.02	1.500	[1]	Santos et al. (2013)
HD 24040	5840	4.30	1.14	0.20	5.36	1.09	1.17	0.10	4.010	[1]	Santos et al. (2013)
HD 27631	5700	4.37	1.00	–0.11	5.99	0.93	<–0.07	–	1.450	[3]	Santos et al. (2013)
HD 96167	5823	4.16	1.28	0.38	4.47	1.22	1.59	0.08	0.680	[3]	Santos et al. (2013)
HD 98649	5714	4.37	1.01	–0.03	4.24	0.96	<–0.54	–	6.800	[3]	Santos et al. (2013)
HD 126614	5601	4.25	1.17	0.50	8.57	0.99	<0.57	–	0.380	[1]	Santos et al. (2013)
HD 129445	5646	4.28	1.14	0.37	4.95	1.00	<0.77	–	1.600	[3]	Santos et al. (2013)
HD 152079	5785	4.38	1.09	0.29	2.98	1.06	<1.00	–	3.000	[2]	Santos et al. (2013)
HD 154672	5743	4.27	1.08	0.25	6.94	1.06	<0.61	–	5.020	[1]	Santos et al. (2013)
HD 170469	5845	4.28	1.17	0.30	4.54	1.09	1.23	0.10	0.670	[1]	Santos et al. (2013)
CoRoT-9	5613	4.35	0.90	–0.02	5.15	0.94	<0.88	–	0.840	[2]	Mortier et al. (2013)
CoRoT-12	5715	4.66	1.07	0.17	4.31	1.01	<1.65	–	0.917	[2]	Mortier et al. (2013)
WASP-5	5785	4.54	0.96	0.17	3.34	1.04	<1.23	–	1.637	[1]	Mortier et al. (2013)
WASP-8	5690	4.42	1.25	0.29	3.22	1.03	1.54	0.15	2.244	[3]	Mortier et al. (2013)
WASP-16	5726	4.34	0.97	0.13	4.43	1.02	<0.62	–	0.855	[2]	Mortier et al. (2013)
WASP-25	5736	4.52	1.11	0.06	3.94	1.00	1.69	0.05	0.580	[2]	Mortier et al. (2013)
WASP-34	5704	4.35	0.97	0.08	5.15	0.99	<0.15	–	0.590	[3]	Mortier et al. (2013)
WASP-56	5797	4.44	1.19	0.43	3.01	1.07	1.65	0.10	0.600	[3]	Mortier et al. (2013)
WASP-63	5715	4.29	1.28	0.28	4.36	1.04	1.45	0.07	0.380	[3]	Mortier et al. (2013)
WASP-77A	5605	4.37	1.09	0.07	5.55	0.95	<0.59	–	1.760	[3]	Mortier et al. (2013)

Notes. The minimum mass of the most massive planet in each system is taken from The Extrasolar Planets Encyclopaedia, Schneider et al. (2011). Flag: [1] UVES; [2] HARPS; [3] FEROS; [4] SARG; [5] CORALIE; [6] NOT; [7] SOPHIE; [8] UES. ^(a) Stars which only host Neptune and Earth-like planets.

Corot-2 (Alonso et al. 2008), as well as subgiants or slightly evolved stars such as HD 118203 and HD 149143 (da Silva et al. 2006), HD 38529 (Fischer et al. 2001), HD 48265 (Minniti et al. 2009), HD 175167 (Arriagada et al. 2010), and HD 219828 (Melo et al. 2007). Some of these stars have been included by other authors (Gonzalez et al. 2010; Ghezzi et al. 2010; Ramírez et al. 2012) in previous works about Li depletion and planets; however, we prefer to discard them since they are in different evolutionary stages. For instance, a subgiant with solar T_{eff} had

a higher temperature when it was on the MS and thus different Li content.

We want to stress that our comparison sample of single stars is formed by stars that have been surveyed over years (with some of the most precise planet search projects) and no planets have been detected so far. We are confident that most of those stars do not host nearby giant planets. We cannot rule out that most of single stars in our sample host low-mass planets that are below the detection capabilities of HARPS. It is also possible that

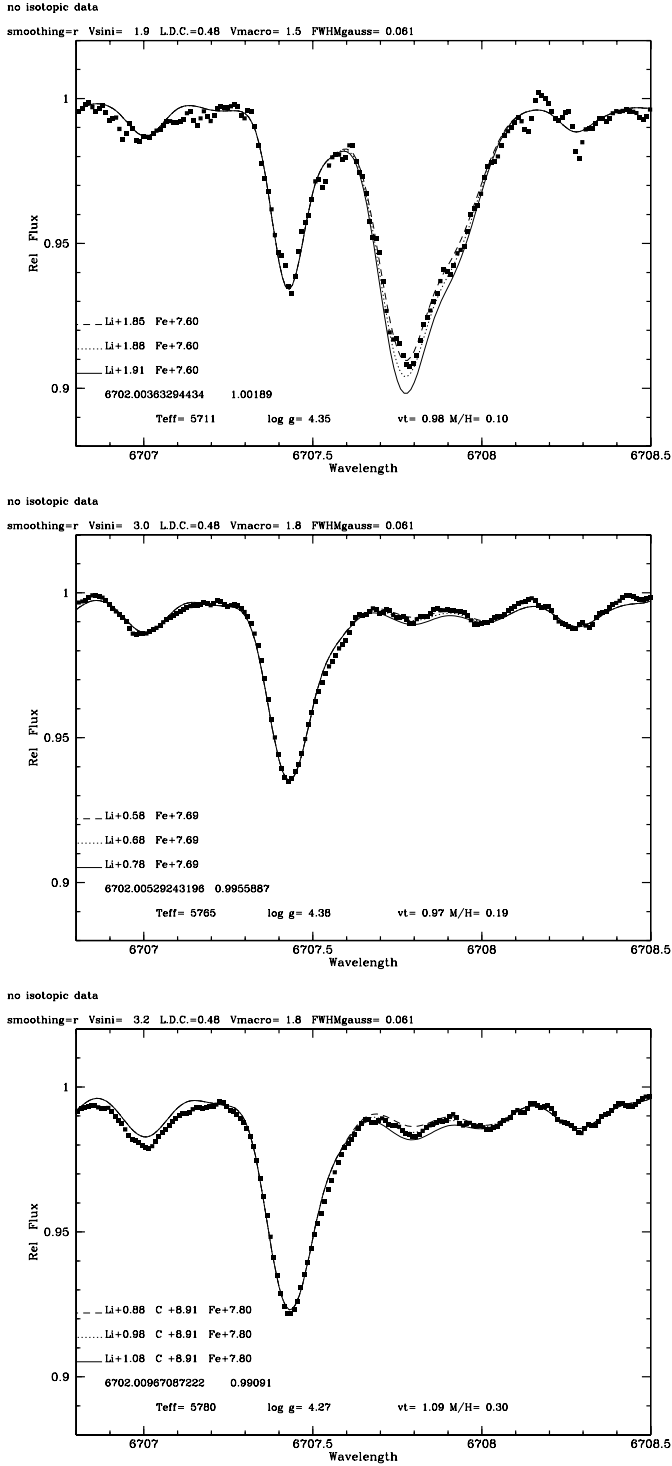


Fig. 1. Spectral synthesis around the Li region for the stars HD 96423, HD 1461, and HD 160691.

some of these stars have long-period giant planets yet to be discovered. This is an important point, since some earlier studies (Ryan 2000; Chen & Zhao 2006; Luck & Heiter 2006; Gonzalez et al. 2010; Baumann et al. 2010; Ramírez et al. 2012) were using field stars as single stars not included in planet-search surveys, but they could have giant planets and thus are not the best targets to be used as real comparison stars. We also point that by keeping the comparison sample from HARPS and adding more planet hosts from other surveys, our results will be statistically

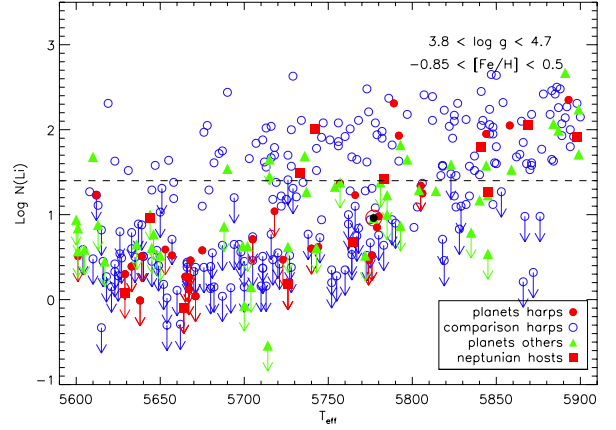


Fig. 2. Lithium abundances vs. T_{eff} for planet host stars (red filled circles) and single stars (blue open circles) from HARPS, together with other planet hosts (green triangles). Squares are stars that only host Neptunian- or Super-Earth-type planets. Down arrows represent $A(\text{Li})$ upper limits. The straight line at $A(\text{Li}) = 1.4$ matches the upper envelope of the lower limits for most of our stars.

more significant. Nevertheless, we differentiate those stars in the plots to show that we still keep the homogeneity of the study.

4.1. Li and log g: cleaning the sample from evolved stars

Our sample is mainly composed of G dwarfs with $\log g$ values between 4.1 and 4.6 (Fig. 3). There are several stars with $\log g$ values between 4.1 and 4.2 with high Li abundances, opposite to what is expected by the general trend starting at 4.2 dex. This has already been noticed in Baumann et al. (2010). Indeed, all the giant planet hosts with high Li have low $\log g$ values except HD 9446 ($T_{\text{eff}} = 5793$ K, $A(\text{Li}) = 1.82$), and HD 181720 ($T_{\text{eff}} = 5792$ K, $A(\text{Li}) = 1.93$). This last planet host has $\log g = 4.25$ but $L = 2.65 L_{\odot}$ and an age of 11.2 Gyr, thus it is possible that this star is entering the subgiant phase. The general trend in Fig. 3 shows a decrease in Li abundances with decreasing $\log g$ in the range $4.2 < \log g < 4.7$, since these stars with lower $\log g$ are older and have had more time to deplete their Li. If we split this plot into different metallicity bins we still observe this effect.

To check the evolutionary status of those stars we plot them in an HR diagram, together with some evolutionary tracks from Bertelli et al. (2008) and Girardi et al. (2000). The luminosity was computed by considering the HIPPARCOS parallaxes, V magnitude, and the bolometric correction as in Sousa et al. (2008). In Fig. 4 we can see that those stars with lower $\log g$ values have much higher luminosities on average and thus may be slightly evolved from the MS. The higher Li abundances of these stars could be explained by the fact that they were hotter when they were on the MS and so did not deplete so much Li. Moreover, there are claims (Deliyannis et al. 1990) that such early evolution may bring up Li to the photosphere in subgiant stars from a reservoir (hidden below the base of the convective envelope) that could have been formed due to microscopic diffusion during the lifetime in the MS. Therefore, to avoid these possibly evolved stars, we restrict our study to stars with higher $\log g$ values, and more specifically to stars with $\log g = \log g_{\odot} \pm 0.2$, as showed in Fig. 3. We note that 81% of our stars with $T_{\text{eff}} = T_{\odot} \pm 80$ K also have $\log g = \log g_{\odot} \pm 0.2$. We will call this subsample “solar analogues” (see Table 2).

⁹ $\log g_{\odot} = 4.44$ dex

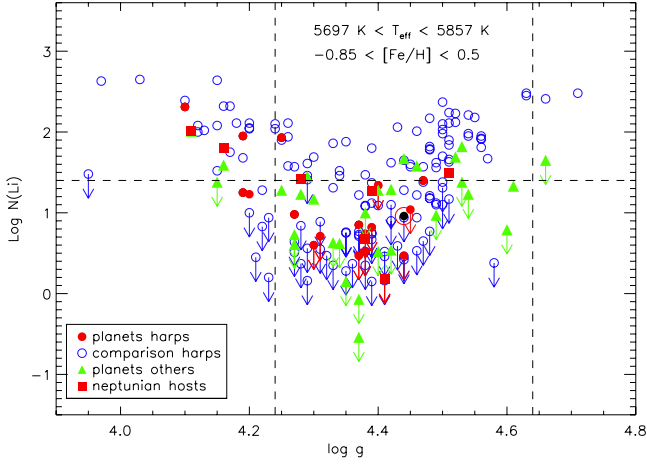


Fig. 3. Lithium abundances vs. $\log g$ for solar type stars. Symbols as in Fig. 2. The vertical lines denote the range in $\log g$ for our solar analogues and solar twins.

4.2. Li and T_{eff}

In Fig. 5 we plot the final sample of solar analogues (see Table 2). We have made a cutoff in $[\text{Fe}/\text{H}] = -0.6$ because our most metal-poor planet host has a metallicity of -0.53 . In any case, only 10% of our single stars within solar T_{eff} and $\log g$ range have $[\text{Fe}/\text{H}] < -0.6$. This sample of solar analogues is composed of 43 planet hosts (including the Sun), from which only eight (i.e. $<19\%$) have Li abundance higher than 1.4. These stars have ages from 2 to 11 Gyr and metallicities from -0.53 to 0.43. All of them except HD 9446 have planets with masses lower than Jupiter’s (see Sect. 4.7).

On the other hand, there are 99 stars without known giant planets, from which 47% have Li abundances higher than 1.4. Therefore, for this T_{eff} range, there is a clear lack of planet hosts with high Li content. This fact is not caused by a difference in T_{eff} , so the dependence on other parameters will be analysed later. We stress that given the homogeneous nature of the HARPS sample (and CORALIE survey) there is no reason a priori to expect that planet hosts should have lower Li in this domain (see Sect. 4.5). “Single” stars are homogeneously distributed in this plot but planet hosts are not, although all of them have similar temperatures, gravities, and metallicities and are all on the MS.

4.3. Li and $[\text{Fe}/\text{H}]$

In Fig. 6 we show Li abundances as a function of metallicity for what we defined above as solar analogues. Most of the planet hosts present high $[\text{Fe}/\text{H}]$ values, although a few of them reach values lower than -0.5 . The increase in metal opacities in solar-type stars is responsible for the transition between radiative and convective energy transport. Thus, stars with more metals (at a given mass) are expected to have deeper convective envelopes that favour Li depletion, though this assumption might not be correct (Pinsonneault et al. 2001). Therefore, we could first think that the only reason for planet hosts to be Li depleted is that they are metal rich. This might be true for very metal rich stars. We can see in Fig. 6 how above 0.2 dex both stars with and without planets deplete a lot of lithium though we still can detect Li absorption in some stars. This fact suggests that in our solar T_{eff} range, high metallicity is also playing a role in lithium depletion, which could be comparable to the role

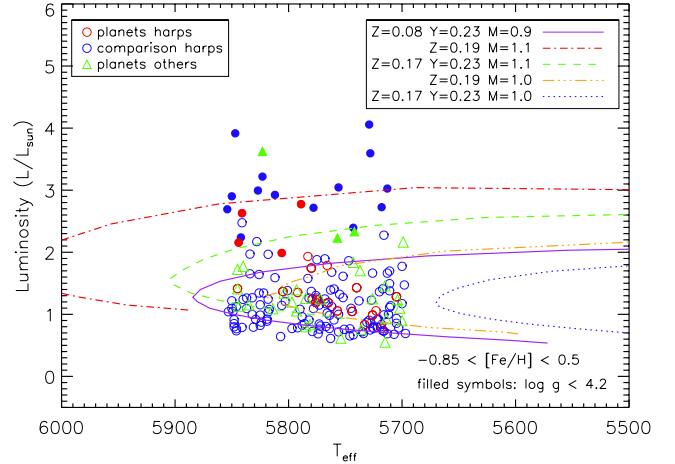


Fig. 4. HR diagram for solar-type stars. Evolutionary tracks are from Girardi et al. (2000); Bertelli et al. (2008). Filled symbols are stars with $\log g$ values lower than 4.2.

of planets, so we cannot extract any conclusion from the most metallic stars. However, we can see in the plot that at lower metallicities most of the planet hosts also present low Li abundances, while single stars are homogeneously spread along high and low Li abundances. Indeed, if we focus on solar twins (metallicities within 0.2 dex of the solar value, see Table 2) only 4 out of 22 planet hosts show Li higher than 1.4, while 29 out of 60 single stars have $A(\text{Li}) > 1.4$. We can also observe that the $[\text{Fe}/\text{H}]$ distribution at low and high Li abundances of both groups is quite homogeneous. We do not find any trend of Li with metallicity in this region ($-0.2 < [\text{Fe}/\text{H}] < 0.2$). Therefore, we can be sure that for solar twins $[\text{Fe}/\text{H}]$ is not playing a major role in the depletion of Li.

4.4. Li and stellar mass

On the main sequence, stellar mass is directly correlated with T_{eff} (with a dependence on $[\text{Fe}/\text{H}]$), i.e. mass increases with T_{eff} , although solar type stars show a wide spread in masses. However, it is not correct to use only mass as a parameter to constrain solar analogues because some stars with masses and $[\text{Fe}/\text{H}]$ close to solar have high temperatures (up to 6000 K) hence fall out of our solar range. We prefer to limit our sample by their T_{eff} since it is a parameter directly observed and its determination has lower uncertainties than the determination of mass, which in turn depends on the uncertainties of the stellar parameters and metallicity and lies on the theoretical evolutionary tracks.

We have seen in the previous section that to discard a metallicity effect on Li abundances we have to exclude metal rich stars ($[\text{Fe}/\text{H}] > 0.2$) from our sample. On the other hand, at $[\text{Fe}/\text{H}] < -0.2$ there are only four planet hosts, so in the following, we focus on what we define as solar twins (see Table 2). In Fig. 7 we present the Li relation with mass for solar twin stars in two metallicity regions. In general, the stars are homogeneously spread at several masses regardless of their Li depletion at both metallicity ranges though the average mass of planet hosts is higher due to their higher average $[\text{Fe}/\text{H}]$. We can also observe that stars with similar masses in each metallicity region present a high dispersion in Li abundances. All the planet hosts with higher Li abundances are situated in the metal-rich panel ($0 < [\text{Fe}/\text{H}] < 0.2$), but the average abundance of Li detections, 1.33 dex, is lower than for the single stars, 1.69. Even if we

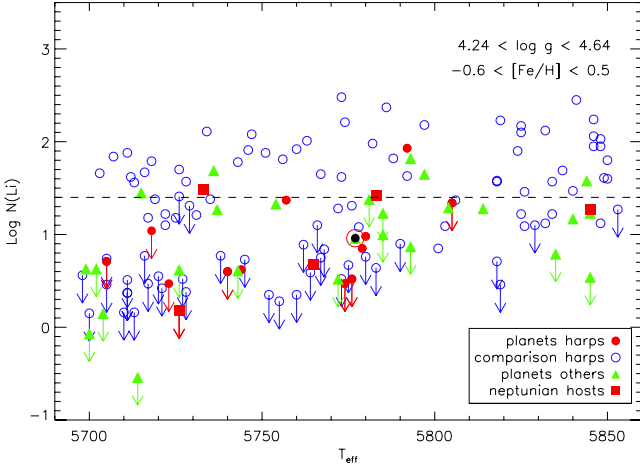


Fig. 5. Lithium abundances vs. T_{eff} for solar analogues. Symbols as in Fig. 2.

remove the younger stars (<1.5 Gyr), single stars have on average 0.30 dex higher abundances (1.33 vs. 1.63, see Sect. 4.5 and Table 5 for further discussion about the Li dependence on age). For the lower metal-poor region ($-0.2 < [\text{Fe}/\text{H}] < 0$), the difference is more obvious. Here we find that the average of Li detections for planet hosts is 1.02, whereas for single stars it is 1.79. If we discard young stars (<1.5 Gyr), the difference is practically the same. This result does not depend on stellar mass. We do not find any trend in Li abundances with this parameter, and the average masses of both samples are very similar (see Table 5).

This spread has been noticed in previous works, such as Pace et al. (2012), where they show how Li abundances do not depend on mass for solar type stars (one solar mass or lower) in M67, and they suggest that an extra variable, in addition to mass, age, and metallicity, is responsible for the scatter in Li abundances, since those stars are very similar. A similar spread in Li is observed for field stars around one solar mass and $-0.2 < [\text{Fe}/\text{H}] < 0$ in Lambert & Reddy (2004). Looking at these plots, it is very clear that planet hosts have destroyed more Li regardless of their T_{eff} , mass, or metallicity, so that another parameter must exist that explains this trend.

4.5. Li and age

Some previous works have claimed that the observed Li depletion in planet hosts is a consequence of the evolution of the star (e.g. Baumann et al. 2010) and thus depends on age. Therefore, if planet hosts were systematically older than single stars that might be the reason for their lower Li abundances. We want to emphasize that for stars with ages between 1.5 and 8 Gyr, the width of spectral lines do not change considerably since $v \sin i$ is nearly constant during MS (e.g. Pace & Pasquini 2004). Therefore, for radial velocity surveys, these are all good targets for precise planet searches regardless of their age. We agree that Li is destroyed as the star gets older, but this depletion takes place principally during the first 1 Gyr (Randich 2010) (if we consider logarithmic abundances) and depends on initial rotation rates (e.g. Charbonnel & Talon 2005), whereas after 1–2 Gyr the age effect is not so strong. For instance, the models by Deliyannis & Pinsonneault (1997), which include rotational induced mixing, show Li abundances of ~ 2.9 dex, ~ 2.1 dex, and ~ 1.7 dex at ages of 100 Myr, 1.7 Gyr, and 4 Gyr, respectively, for a star with $T_{\text{eff}} = 5800$ K and initial rotation

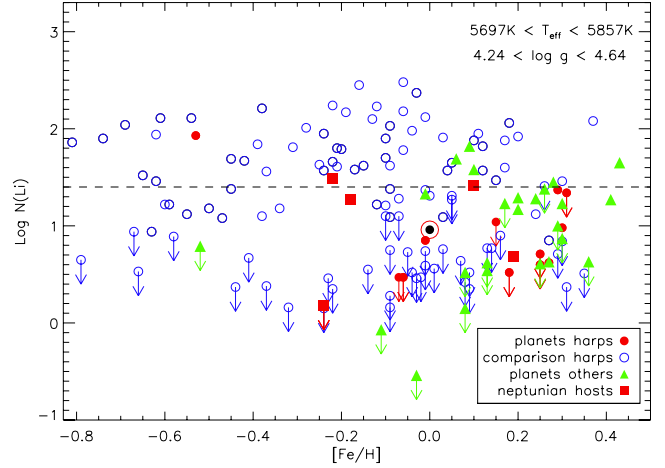


Fig. 6. Lithium abundances vs. $[\text{Fe}/\text{H}]$ for solar analogues. Symbols as in Fig. 2.

$v \sin i = 10 \text{ km s}^{-1}$. Furthermore, if age were the principal cause of Li depletion, we would not observe such a dispersion (~ 1.3 dex) in Li abundances for stars in the same evolutionary status in clusters like M67, where all the stars have the same age and metallicity (Pasquini et al. 2008; Randich et al. 2009; Pace et al. 2012). In the clusters NGC 3960 (Prisinzano & Randich 2007), Collinder 261 (Pallavicini et al. 2005), and NGC 6253 (Randich 2010), a Li dispersion in solar type stars was found as well, though not as large as in M67. On the other hand, the near solar metallicity cluster NGC 188 of 6–8 Gyr present abundances 10–20 times higher than in the Sun (Randich et al. 2003).

In the left-hand panel of Fig. 8 we explore the relation of Li with age for solar twins. We observe that there is no a tight relation with age except for very young ages. Furthermore, we can find young stars with low Li abundances, as well as old stars with higher abundances. Both groups of stars are spread over the entire range of ages, though at younger ages (0–2 Gyr) there are more single stars than planet hosts. This is likely due to the higher difficulties in finding planets around young, active stars. In order to test this correlation, we computed a generalized Kendall's tau correlation coefficient considering upper limits of Li. This was done with the program R and the function *cenken*, which can be used with censored data (Akritas et al. 1995). This test gives $\tau = 0.138$ (with a probability of 0.63 of having a correlation) for planet hosts and $\tau = -0.004$ for single stars (with $P = 0.03$ of having a correlation). Therefore, this test shows that there is no a clear relationship between Li and age. However, if we only deal with the Li detections τ decreases to -0.24 for both groups, with a higher probability of correlation for single stars, 0.96 vs. 0.63 for planet hosts.

In the right-hand panel of Fig. 8 we can observe the same plot but split in two mass ranges, $0.89\text{--}1.0 M_{\odot}$ and $1.0\text{--}1.1 M_{\odot}$. In the more massive subsample (red symbols) we can only find detections of Li for single stars at ages <3 Gyr, so we cannot compare stars at older ages. However, in that age bin (0–3 Gyr), none of the planet hosts can reach the average of Li for single stars. On the other hand, the number of stars is higher in the less massive subgroup (purple symbols). Planet hosts are spread at different ages, but in general present lower Li abundances than the single stars of similar ages. In any case, the stars of both mass subgroups might not be very different considering typical errors in mass of $0.1 M_{\odot}$ (e.g. Casagrande et al. 2007; Fernandes et al. 2011). In addition, we show in the previous section that for solar twins ($0.9\text{--}1.1 M_{\odot}$), Li does not depend on

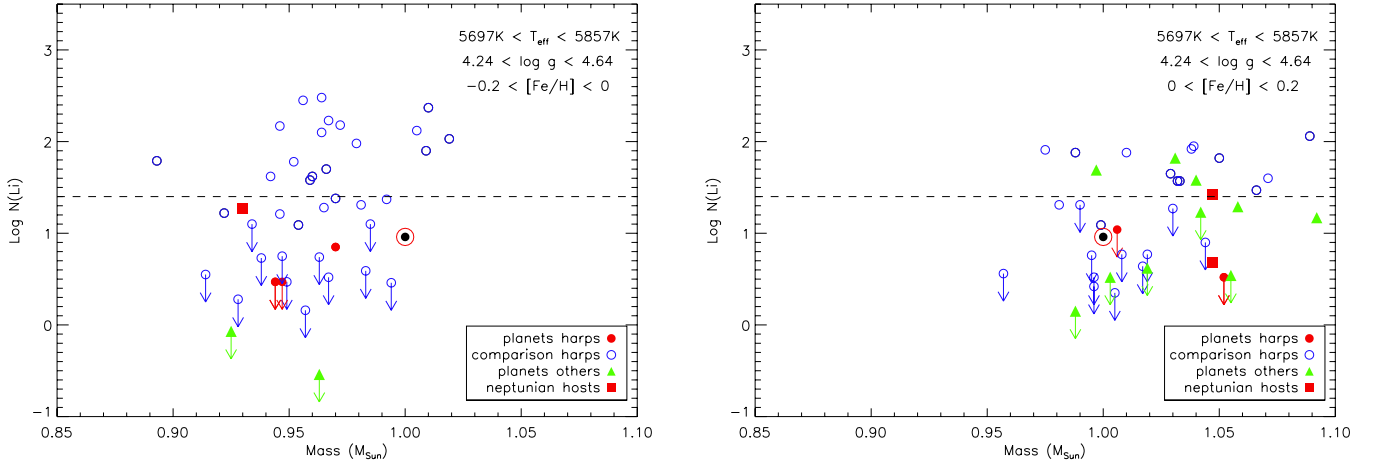


Fig. 7. Lithium abundances vs. mass for solar twins at $[\text{Fe}/\text{H}] < 0$ (left panel) and solar twins at $[\text{Fe}/\text{H}] > 0$ (right panel). Symbols as in Fig. 2.

Table 5. Mean values of parameters, together with standard error of the mean, for different subsamples, all of them with $T_{\text{eff}} = T_{\odot} \pm 80$ K, and $\log g = \log g_{\odot} \pm 0.2$.

Group	Number	$[\text{Fe}/\text{H}]$ range	Age range Gyr	T_{eff} (K)	$[\text{Fe}/\text{H}]$	$\log g$ (cm s^{-2})	Mass M_{\odot}	Age Gyr	Li detections $A(\text{Li})$
A	10 PH	$[-0.2, 0.2]$	$[1.5, 12]$	5797 ± 12	0.07 ± 0.04	4.41 ± 0.03	1.02 ± 0.01	5.14 ± 0.82	1.27 ± 0.12
A	30 CS	$[-0.2, 0.2]$	$[1.5, 12]$	5783 ± 8	-0.04 ± 0.02	4.47 ± 0.02	0.98 ± 0.01	4.01 ± 0.44	1.75 ± 0.07
B	5 PH	$[-0.2, 0.2]$	$[4, 12]$	5805 ± 15	0.02 ± 0.06	4.36 ± 0.03	1.01 ± 0.03	7.03 ± 1.04	1.13 ± 0.10
B	11 CS	$[-0.2, 0.2]$	$[4, 12]$	5768 ± 15	-0.07 ± 0.03	4.40 ± 0.02	0.96 ± 0.01	6.63 ± 0.62	1.48 ± 0.10
C	3 PH	$[-0.2, 0]$	$[1.5, 12]$	5800 ± 22	-0.06 ± 0.06	4.40 ± 0.02	0.97 ± 0.02	7.50 ± 1.74	1.03 ± 0.12
C	22 CS	$[-0.2, 0]$	$[1.5, 12]$	5778 ± 9	-0.09 ± 0.01	4.47 ± 0.02	0.96 ± 0.01	4.33 ± 0.53	1.77 ± 0.09
D	3 PH	$[-0.2, 0]$	$[4, 12]$	5800 ± 22	-0.06 ± 0.06	4.40 ± 0.02	0.97 ± 0.02	7.50 ± 1.74	1.03 ± 0.12
D	9 CS	$[-0.2, 0]$	$[4, 12]$	5770 ± 17	-0.10 ± 0.02	4.41 ± 0.03	0.95 ± 0.01	6.72 ± 0.76	1.48 ± 0.11
E	8 PH	$[0, 0.2]$	$[1.5, 12]$	5793 ± 13	0.12 ± 0.03	4.42 ± 0.03	1.04 ± 0.01	4.17 ± 0.58	1.33 ± 0.13
E	9 CS	$[0, 0.2]$	$[1.5, 12]$	5795 ± 16	0.09 ± 0.02	4.45 ± 0.03	1.02 ± 0.01	3.58 ± 0.10	1.63 ± 0.10
F	3 PH	$[0, 0.2]$	$[4, 12]$	5800 ± 20	0.10 ± 0.06	4.34 ± 0.05	1.05 ± 0.02	5.72 ± 0.83	1.18 ± 0.13
F	3 CS	$[0, 0.2]$	$[4, 12]$	5763 ± 27	0.04 ± 0.03	4.36 ± 0.02	0.99 ± 0.01	6.54 ± 0.34	1.43 ± 0.24
G	8 PH	$[-0.25, 0.15]$	$[1.5, 12]$	5786 ± 15	-0.01 ± 0.04	4.44 ± 0.03	0.99 ± 0.02	5.85 ± 1.07	1.38 ± 0.12
G	35 CS	$[-0.25, 0.15]$	$[1.5, 12]$	5789 ± 8	-0.09 ± 0.02	4.46 ± 0.02	0.96 ± 0.01	4.52 ± 0.50	1.75 ± 0.07
H	5 PH	$[-0.25, 0.15]$	$[4, 12]$	5783 ± 18	-0.06 ± 0.06	4.40 ± 0.04	0.97 ± 0.03	7.65 ± 0.98	1.20 ± 0.13
H	16 CS	$[-0.25, 0.15]$	$[4, 12]$	5779 ± 14	-0.12 ± 0.03	4.40 ± 0.02	0.95 ± 0.01	6.87 ± 0.57	1.53 ± 0.07
I	4 PH	$[-0.25, 0.15]$	$[5, 12]$	5785 ± 23	4.39 ± 0.05	-0.08 ± 0.08	8.45 ± 0.74	0.96 ± 0.03	1.26 ± 0.14
I	12 CS	$[-0.25, 0.15]$	$[5, 12]$	5777 ± 17	4.38 ± 0.02	-0.12 ± 0.03	7.73 ± 0.57	0.94 ± 0.01	1.52 ± 0.08

Notes. Metallicity and age ranges (which include the boundaries) are indicated in the table. PH and CS denote planet hosts (from HARPS and other spectrographs) and comparison sample stars, respectively.

mass, even in narrower metallicity ranges, so mixing all those in the same plot (left panel of Fig. 8) will not affect our conclusions. Furthermore, we note that when dealing with MS stars, the age determination is probably very uncertain (e.g. [Jørgensen & Lindegren 2005](#)), at least significantly more uncertain than the mass determination.

Finally, in Fig. 9 we depict the average of Li detections for solar twins in different age bins. We can observe a decrease in Li abundances for solar age stars with respect to younger objects but stars with planets always present lower Li abundances in each age bin for ages < 8 Gyr. At older ages, we only have three objects so we do not contemplate those age bins.

In Table 5 we summarize the average values of parameters in several subsamples already discussed. We note that Li averages are calculated with only detections since for upper limits we cannot know the real content of Li. We discard the younger stars (< 1.5 Gyr) to avoid a comparison sample that is too biased towards low ages. For the solar twins ($-0.2 < [\text{Fe}/\text{H}] < 0.2$,

group A in the table) the single stars present Li abundances nearly 0.5 dex higher than planet hosts and only the planet host HD 9446 present a Li abundance higher than the average for single stars. This difference in mean Li is higher than 3.4σ (two side t-test), whereas the difference for age is 1.2σ . For older stars (> 4 Gyr, group B), the difference is also high, 0.35 dex, but in this case none of the planet hosts reach $A(\text{Li}) = 1.48$. The planet host group has higher average $[\text{Fe}/\text{H}]$, but that difference in metallicity is not enough to explain the difference in Li as already discussed in previous sections. Moreover, [Pinsonneault et al. \(2001\)](#) show that the mass of the convective envelope (responsible for the degree of Li depletion) hardly varies for a wide range of metallicities at a given T_{eff} . Nevertheless, we find different Li abundances if we split the solar twins into two metallicity regions.

In the less metallic group ($-0.2 < [\text{Fe}/\text{H}] < 0$), “single” stars are very biased towards young ages (group C) so we must only take older stars (group D) into account. For the more metallic

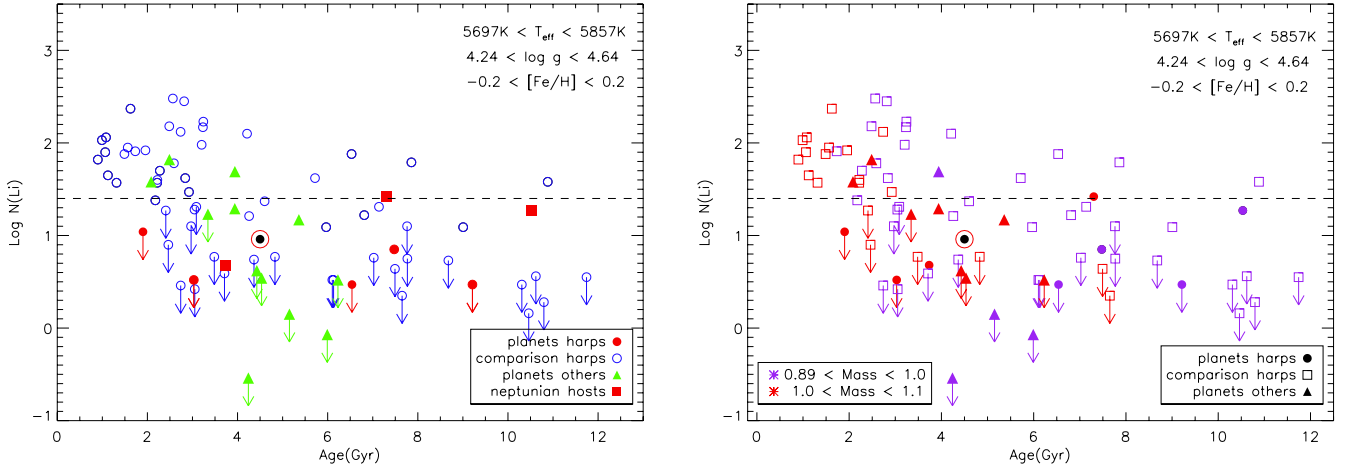


Fig. 8. Lithium abundances vs. age for solar twins (*left panel*) and for solar twins with colours denoting different mass ranges (*right panel*).

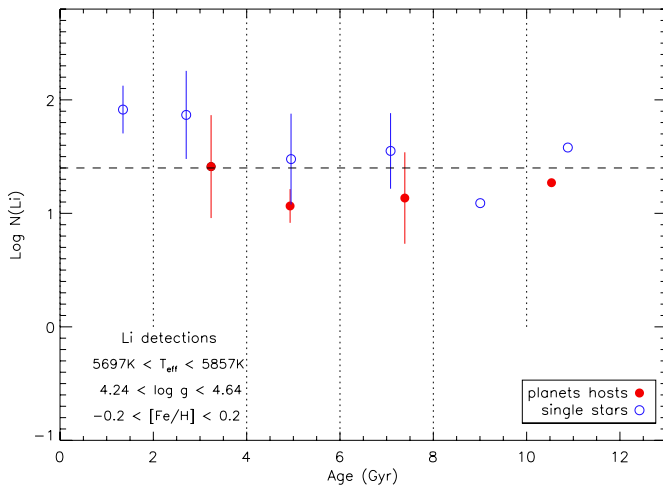


Fig. 9. Average of Li detections for solar twins in different age bins. The points in each bin are situated in their average age. The bars indicate the dispersion in Li abundances if there are more than one star in each bin.

stars (groups E and F), the mean ages and metallicities are more similar in the younger subsample (group E), and we find a difference of 0.3 dex in Li abundance. Planet hosts are also slightly older on average (~ 1 Gyr) in most of the subsamples, but the difference is at the level of the errors, and as we already pointed out, the main destruction of Li occurs before 1–2 Gyr. Since we are not considering those young objects, the slight difference in average ages cannot justify the big differences in Li. We also look at a subsample of solar twins shifted to lower metallicities ($[\text{Fe}/\text{H}] = -0.05 \pm 0.2$, groups G and H), and the difference in Li abundances is quite similar, 0.43 and 0.33 dex for the groups with ages >1.5 Gyr and >4 Gyr, respectively. In order to find more similar populations regarding age and metallicity we analysed an older subsample: group I. The differences in average $[\text{Fe}/\text{H}]$ and age are similar to group H, 0.04 dex, and 0.7 Gyr, respectively, while the Li difference is decreased to 0.26 dex. This suggests that for older ages, it is more difficult to detect differences, though the number of stars in this subsample is significantly lower and thus the statistical inferences might be less reliable.

With the aim of increasing the number of stars in our sample we applied survival statistics to several subsamples from Table 5, which allows information to be extracted from the upper limits.

We used the package ASURV (Feigelson & Nelson 1985), which provides the Kaplan-Meier estimator of the mean and several two-sample tests. For the group A, four out of five tests give probabilities lower than 0.06 that the samples of planets hosts and “single” stars come from the same parent population. The Kaplan-Meier estimator of the mean is 0.361 ± 0.208 for planets hosts and 1.069 ± 0.116 for stars without planets, hence it seems these two samples are really distinct. For the older solar twins (group B), however all the two-sample tests give probabilities between 0.4–0.6. The K-M estimator of the mean for planet hosts is 0.104 ± 0.229 and for stars without detected planets it is 0.722 ± 0.135 . Therefore for this subgroup there is no clear difference. For the solar twins sample at lower $[\text{Fe}/\text{H}]$ (group G), we find similar results as for group A, with probabilities around 0.08 that the samples are drawn from the same population. The K-M estimators of the mean are 0.330 ± 0.233 and 1.094 ± 0.109 for planet hosts and “single” stars, respectively, thus these subsamples appear to be different. For the older stars (group H), the two-sample test probabilities increase to 0.2 but the K-M estimators of the mean are still quite different (0.081 ± 0.226 vs. 0.804 ± 0.123). For the group I the two-sample test probabilities increase to 0.55 (and the K-M estimators of the mean are more similar) suggesting that the possible effect of planets might be diluted for very old stars as pointed out before.

These tests including upper limits and the values from detections shown in Table 5 indicate that there seems to be a different distribution of Li abundances for planet hosts. However, depending on the building of the subsamples and the restrictions applied to age and metallicity, the results can be different, maybe owing to the low number of stars in each subsample. Therefore, a bigger sample with more similar stars would be desirable to fully confirm this distinction.

4.6. Testing the differences with observed spectra

In Fig. 10 several pairs of stars with very similar parameters are depicted. The stars in each pair have maximum differences of 40 K, 0.06 dex, 0.2 dex, 0.06 M_{\odot} , and 1 Gyr for T_{eff} , $[\text{Fe}/\text{H}]$, $\log g$, mass, and age, respectively. These plots are a definitive demonstration that other parameters are affecting Li depletion, otherwise we would not be able to explain the difference in Li line for these almost twins stars (in each pair). The difference between parameters is about 1σ , while difference in Li abundances goes from 0.3 dex (more than 3σ) to more than 1.5 dex

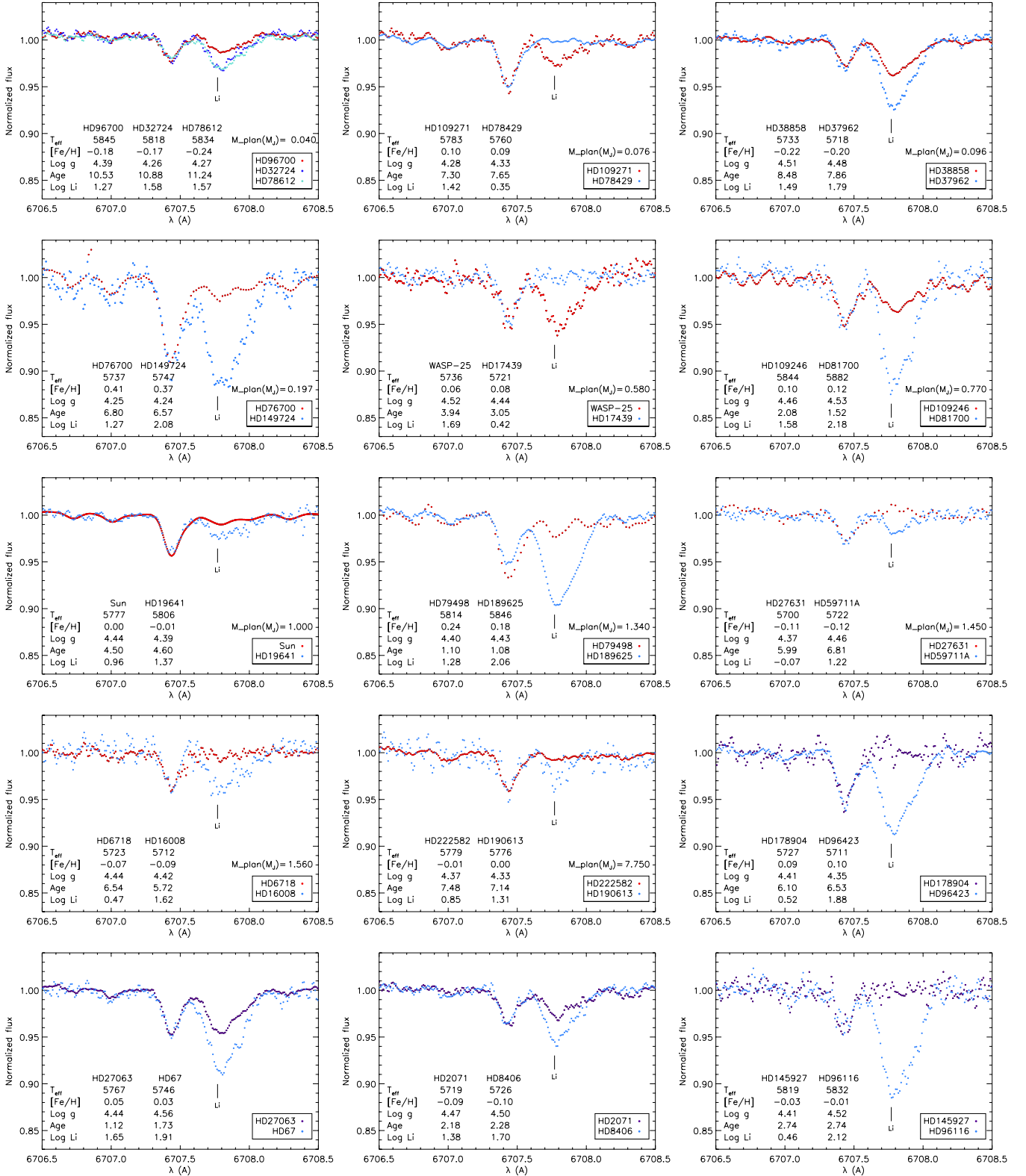


Fig. 10. Observed spectra for couples of stars with very similar parameters and different Li abundances. Planet hosts spectra are depicted with red dots and stars without known planets are depicted with blue or purple dots. For the couples with a planet host the minimum mass of the most massive planet in each system is indicated in the plot.

for the pair with HD 145927 and HD 96116 in which the two stars have the same age. We can find couples in which both stars do not have known planets (but present a quite distinct degree of Li depletion), and we can also find couples in which the planet

host has a Li abundance higher than the single star. However, all those planet hosts (except HD 9446) have smaller planets (see next section). Indeed, it is easy to detect the Li absorption in some of those stars with smaller planets but when you move to

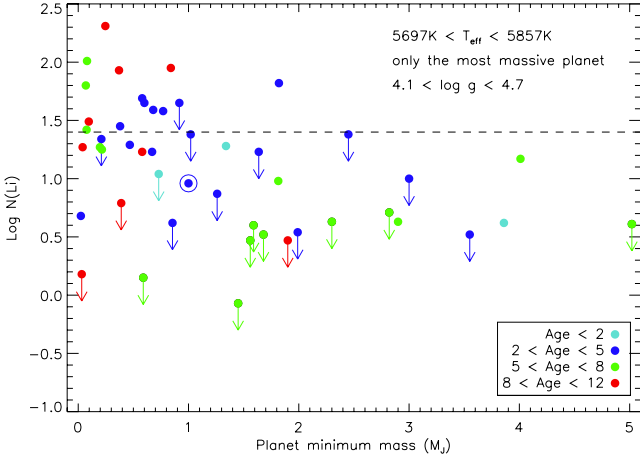


Fig. 11. Lithium abundances vs. minimum planetary masses for the most massive planet in each system. Colours denote different age ranges.

planetary masses higher than that of Jupiter, the Li line almost disappears. Regardless of the presence of planets, these huge differences in Li cannot be justified with the observed differences in stellar parameters.

Consequently, we can conclude that neither mass, age, nor metallicity can be the only cause of the extra Li depletion for our solar analogues. Other mechanisms such as rotationally induced mixing or overshooting mixing should be considered.

4.7. Li and planetary parameters

We also searched for any possible relation of previously shown Li depletion with the physical and orbital parameters of the planets, that is, mass, period, eccentricity and semi-major axis. We did not find any dependence except possibly on the planetary mass. In Fig. 11 we plot the Li abundances as a function of the more massive planet in each system. We note that using the sum of masses of all the planets in each system produces a similar plot. It seems that the destruction of Li is higher when the planet is more massive. This would make sense in a scenario where the disc is affecting the evolution of angular momentum, hence mixing mechanisms (Bouvier 2008), since we could expect a stronger effect if the disc is more massive and has a longer lifetime, conditions needed to form a giant planet. In fact, all the stars with planets more massive than Jupiter (except HD 9446) have depleted their Li significantly. Furthermore, the accretion processes are expected to be more frequent and violent when there is a giant planet in the disc and, as a consequence, produce Li destruction either by the increase in temperature on the base of the convective envelope (Baraffe & Chabrier 2010) or by extra-mixing triggered by thermohaline convection (Théado & Vauclair 2012).

In Fig. 11 we only constrain the T_{eff} of the stars but not their $\log g$ or $[\text{Fe}/\text{H}]$ so some of the planet hosts with higher Li abundances have low $\log g$ and might be slightly evolved. In fact, the planet hosts with higher Li detections are older than 5 Gyr, and half of them are older than 8 Gyr. As discussed in previous sections this might be the reason for the high Li abundance and not the mass of the planet, but what is certain is that all the stars with planets within solar $\log g$ range and high Li abundances host less massive planets. Therefore, the mass of the disc in those systems would not be enough to affect the stellar angular momentum evolution or to produce intense accretion episodes and thus, those

stars would present a different degree of Li depletion depending on other parameters. We could say that those planet hosts behave in a similar way to stars without planets, since some of them have destroyed their Li, but others have not and the mechanism responsible for depleting it should be other than the presence of planets. We should also take into account that most of the Li abundances are upper limits so we can just conclude that Li is severely depleted at least when the planet is massive enough. To extract the information of upper limits, we computed the Kendall's tau correlation coefficient for censored data as done before. This test gives $\tau = 0.016$ (with $P = 0.12$), which means there is no correlation. If we only consider the detections, τ decreases to -0.215 (with $P = 0.87$), pointing to a possible correlation, but the result is not significant enough. Nevertheless, we think that this plot shows an interesting relation and should be considered in further studies of Li abundances when the number of low-mass planet hosts increases.

5. Conclusions

We have presented Li abundances in a large sample of planet hosts and single stars in the effective temperature range $5600 \text{ K} < T_{\text{eff}} < 5900 \text{ K}$. 42 planet hosts and 235 single stars come from HARPS GTO sample, while 49 other planet hosts have been observed with other instruments. We find that the average Li abundance for single stars is greater than for the planet hosts. This difference is more obvious when we look at solar twins with $T_{\text{eff}} = T_{\odot} \pm 80 \text{ K}$, $\log g = \log g_{\odot} \pm 0.2$, and $[\text{Fe}/\text{H}] = [\text{Fe}/\text{H}]_{\odot} \pm 0.2$ where only 18% of planet hosts show detections of $A(\text{Li}) > 1.4$ whereas for single stars this value reaches 48% confirming previous studies (e.g. Israelian et al. 2009; Gonzalez et al. 2010; Takeda et al. 2010; Sousa et al. 2010).

We checked whether our abundances depend on other parameters, such as mass, age, or metallicity. We find that most of our stars at very high metallicities present low Li content regardless of the presence of planets. On the other hand, if planet hosts were much older than the single stars, we might expect that to be the reason of the extra depletion since Li shows a small decrease with age as observed in open clusters of several ages (Sestito & Randich 2005). After removing the younger objects (age < 1.5 Gyr), we showed that planet hosts are around 1 Gyr older on average, but this small age difference cannot be responsible for the large difference in Li abundances (more than 3σ) found between stars with and without planets. However, some statistical tests, including the Li upper limits, show that both populations might be not so different depending on the ranges in age and $[\text{Fe}/\text{H}]$ used to define the subsamples. On the other hand, we show several examples of couples formed by twins with huge differences in abundance, up to 1.6 dex. Therefore, we suggest that the presence of giant planets (among other possible causes) might affect the Li content in solar twins.

The dispersion of Li abundances in stars of similar T_{eff} , mass, age, and metallicity have also been reported in several open clusters like M67, which represents a good comparison for our observation since it has solar age and metallicity. Moreover, the standard model for stellar evolution, which considers only convection as a mixing mechanism, cannot explain the extra Li depletion found in old stars (regardless of the presence of planets) during the MS. Therefore, there must be non-standard processes that produce this effect, so we propose that the presence of planets is one of them. For instance, the stars with low Li in M67 might have planets that have not been discovered yet. Indeed, two of the planet candidates proposed in this cluster by Pasquini et al. (2012) have T_{eff} in our solar range and present

low Li abundances (Pasquini et al. 2008). However we also find stars without detected planets which are heavily depleted in Li; as a result other mechanisms such as rotationally induced mixing (Pinsonneault et al. 1990) must also be considered. In fact, this kind of mixing is related to the initial rotation rates and angular momentum evolution of the star and thus has a strong connection with protoplanetary discs. Therefore, the presence of a planetary disc may be one of the causes to produce this kind of mixing. In addition, planets can also cause an extra Li depletion through other mechanisms such as violent accretion-burst episodes of planetary material. Both mechanisms produce a stronger effect when the protoplanetary discs are more massive, in agreement with our finding that Li is always destroyed if the star hosts a giant planet.

Acknowledgements. E.D.M., S.G.S., and V.Zh.A. acknowledge the support from the Fundação para a Ciência e Tecnologia, FCT (Portugal) in the form of the fellowships SFRH/BPD/76606/2011, SFRH/BPD/47611/2008, and SFRH/BPD/70574/2010 from the FCT (Portugal), respectively. G.I. and J.I.G.H. acknowledge financial support from the Spanish Ministry project MINECO AYA2011-29060, and J.I.G.H. also from the Spanish Ministry of Economy and Competitiveness (MINECO) under the 2011 Severo Ochoa Program MINECO SEV-2011-0187. E.D.M., S.G.S., N.C.S., A.M., and V.Zh.A. are grateful for the support by the European Research Council/European Community under the FP7 through Starting Grant agreement number 239953, as well as the support through programme Ciência 2007 funded by FCT/MCTES (Portugal) and POPH/FSE (EC), and in the form of grant PTDC/CTE-AST/098528/2008. We thank Pedro Figueira and the referee for useful comments and suggestions that helped improve the paper. This research has made use of the SIMBAD database operated at the CDS, Strasbourg (France) and the Encyclopaedia of Extrasolar Planets. This work has also made use of the IRAF facility.

References

- Adibekyan, V. Z., Delgado Mena, E., Sousa, S. G., et al. 2012a, *A&A*, 547, A36
 Adibekyan, V. Z., Santos, N. C., Sousa, S. G., et al. 2012b, *A&A*, 543, A89
 Akritas, M. G., Murphy, S. A., & LaValley, M. P. 1995, *J. Am. Stat. Assoc.*, 90, 170
 Alonso, R., Auvergne, M., Baglin, A., et al. 2008, *A&A*, 482, L21
 Ammler-von Eiff, M., Santos, N. C., Sousa, S. G., et al. 2009, *A&A*, 507, 523
 Arriagada, P., Butler, R. P., Minniti, D., et al. 2010, *ApJ*, 711, 1229
 Baraffe, I., & Chabrier, G. 2010, *A&A*, 521, A44
 Baumann, P., Ramírez, I., Meléndez, J., Asplund, M., & Lind, K. 2010, *A&A*, 519, A87
 Bertelli, G., Girardi, L., Marigo, P., & Nasi, E. 2008, *A&A*, 484, 815
 Boisse, I., Eggenberger, A., Santos, N. C., et al. 2010, *A&A*, 523, A88
 Bonomo, A. S., Hébrard, G., Santerne, A., et al. 2012, *A&A*, 538, A96
 Bouvier, J. 2008, *A&A*, 489, L53
 Casagrande, L., Flynn, C., Portinari, L., Girardi, L., & Jimenez, R. 2007, *MNRAS*, 382, 1516
 Castro, M., Vauclair, S., Richard, O., & Santos, N. C. 2009, *A&A*, 494, 663
 Chaboyer, B., Demarque, P., & Pinsonneault, M. H. 1995, *ApJ*, 441, 865
 Charbonnel, C., & Talon, S. 2005, *Science*, 309, 2189
 Chen, Y. Q., & Zhao, G. 2006, *AJ*, 131, 1816
 Christensen-Dalsgaard, J., Gough, D. O., & Thompson, M. J. 1991, *ApJ*, 378, 413
 da Silva, R., Udry, S., Bouchy, F., et al. 2006, *A&A*, 446, 717
 Deliyannis, C. P., & Pinsonneault, M. H. 1997, *ApJ*, 488, 836
 Deliyannis, C. P., Demarque, P., & Kawaler, S. D. 1990, *ApJS*, 73, 21
 Eggenberger, P., Maeder, A., & Meynet, G. 2010, *A&A*, 519, L2
 Eggenberger, P., Haemmerlé, L., Meynet, G., & Maeder, A. 2012, *A&A*, 539, A70
 Feigelson, E. D., & Nelson, P. I. 1985, *ApJ*, 293, 192
 Fernandes, J. M., Vaz, A. I. F., & Vicente, L. N. 2011, *A&A*, 532, A20
 Fischer, D. A., & Valenti, J. 2005, *ApJ*, 622, 1102
 Fischer, D. A., Marcy, G. W., Butler, R. P., et al. 2001, *ApJ*, 551, 1107
 Garud, P. 2011, *ApJ*, 728, L30
 Garcia Lopez, R. J., Rebolo, R., & Martin, E. L. 1994, *A&A*, 282, 518
 Ghezzi, L., Cunha, K., Smith, V. V., et al. 2009, *ApJ*, 698, 451
 Ghezzi, L., Cunha, K., Smith, V. V., & de la Reza, R. 2010, *ApJ*, 724, 154
 Girardi, L., Bressan, A., Bertelli, G., & Chiosi, C. 2000, *A&AS*, 141, 371
 Gonzalez, G. 1997, *MNRAS*, 285, 403
 Gonzalez, G. 2008, *MNRAS*, 386, 928
 Gonzalez, G., & Laws, C. 2000, *AJ*, 119, 390
 Gonzalez, G., Carlson, M. K., & Tobin, R. W. 2010, *MNRAS*, 403, 1368
 Hébrard, G., Bonfils, X., Ségransan, D., et al. 2010, *A&A*, 513, A69
 Israelian, G., Santos, N. C., Mayor, M., & Rebolo, R. 2004, *A&A*, 414, 601
 Israelian, G., Delgado Mena, E., Santos, N. C., et al. 2009, *Nature*, 462, 189
 Jørgensen, B. R., & Lindegren, L. 2005, *A&A*, 436, 127
 King, J. R., Deliyannis, C. P., Hiltgen, D. D., et al. 1997, *AJ*, 113, 1871
 Kurucz, R. 1993, ATLAS9 Stellar Atmosphere Programs and 2 km s⁻¹ grid, Kurucz CD-ROM No. 13 (Cambridge, Mass.: Smithsonian Astrophysical Observatory)
 Kurucz, R. L., Furenlid, I., Brault, J., & Testerman, L. 1984, *Solar flux atlas from 296 to 1300 nm*
 Lambert, D. L., & Reddy, B. E. 2004, *MNRAS*, 349, 757
 Lo Curto, G., Mayor, M., Benz, W., et al. 2010, *A&A*, 512, A48
 Luck, R. E., & Heiter, U. 2006, *AJ*, 131, 3069
 Mayor, M., Pepe, F., Queloz, D., et al. 2003, *The Messenger*, 114, 20
 Melo, C., Santos, N. C., Gieren, W., et al. 2007, *A&A*, 467, 721
 Minniti, D., Butler, R. P., López-Morales, M., et al. 2009, *ApJ*, 693, 1424
 Montalbán, J., & Schatzman, E. 1996, *A&A*, 305, 513
 Montalbán, J., & Schatzman, E. 2000, *A&A*, 354, 943
 Mortier, A., Santos, N. C., Sousa, S. G., et al. 2013, *A&A*, 558, A106
 Pace, G., Castro, M., Meléndez, J., Théado, S., & do Nascimento, Jr., J.-D. 2012, *A&A*, 541, A150
 Pace, G., & Pasquini, L. 2004, *A&A*, 426, 1021
 Pallavicini, R., Randich, S., & Sestito, P. 2005, in *13th Cambridge Workshop on Cool Stars, Stellar Systems and the Sun*, eds. F. Favata, G. A. J. Hussain, & B. Battrick, *ESA SP*, 560, 867
 Pasquini, L., Biazzo, K., Bonifacio, P., Randich, S., & Bedin, L. R. 2008, *A&A*, 489, 677
 Pasquini, L., Brucalassi, A., Ruiz, M. T., et al. 2012, *A&A*, 545, A139
 Pinsonneault, M. 1997, *ARA&A*, 35, 557
 Pinsonneault, M. H., Kawaler, S. D., & Demarque, P. 1990, *ApJS*, 74, 501
 Pinsonneault, M. H., Deliyannis, C. P., & Demarque, P. 1992, *ApJS*, 78, 179
 Pinsonneault, M. H., DePoy, D. L., & Coffee, M. 2001, *ApJ*, 556, L59
 Prisinzano, L., & Randich, S. 2007, *A&A*, 475, 539
 Ramírez, I., Fish, J. R., Lambert, D. L., & Allende Prieto, C. 2012, *ApJ*, 756, 46
 Randich, S. 2010, in *IAU Symp. 268*, eds. C. Charbonnel, M. Tosi, F. Primas, & C. Chiappini, 275
 Randich, S., Aharpour, N., Pallavicini, R., Prosser, C. F., & Stauffer, J. R. 1997, *A&A*, 323, 86
 Randich, S., Sestito, P., & Pallavicini, R. 2003, *A&A*, 399, 133
 Randich, S., Primas, F., Pasquini, L., Sestito, P., & Pallavicini, R. 2007, *A&A*, 469, 163
 Randich, S., Pace, G., Pastori, L., & Bragaglia, A. 2009, *A&A*, 496, 441
 Richer, J., & Michaud, G. 1993, *ApJ*, 416, 312
 Ryan, S. G. 2000, *MNRAS*, 316, L35
 Santos, N. C., Israelian, G., & Mayor, M. 2004, *A&A*, 415, 1153
 Santos, N. C., Israelian, G., Mayor, M., et al. 2005, *A&A*, 437, 1127
 Santos, N. C., Mayor, M., Bonfils, X., et al. 2011, *A&A*, 526, A112
 Santos, N. C., Sousa, S. G., Mortier, A., et al. 2013, *A&A*, 556, A150
 Schneider, J., Dedieu, C., Le Sidaner, P., Savalle, R., & Zolotukhin, I. 2011, *A&A*, 532, A79
 Sestito, P., & Randich, S. 2005, *A&A*, 442, 615
 Setiawan, J., Weise, P., Henning, T., et al. 2007, *ApJ*, 660, L145
 Snedden, C. A. 1973, Ph.D. Thesis, The University of Texas at Austin
 Soderblom, D. R., Jones, B. F., Balachandran, S., et al. 1993, *AJ*, 106, 1059
 Sousa, S. G., Santos, N. C., Israelian, G., Mayor, M., & Monteiro, M. J. P. F. G. 2006, *A&A*, 458, 873
 Sousa, S. G., Santos, N. C., Mayor, M., et al. 2008, *A&A*, 487, 373
 Sousa, S. G., Fernandes, J., Israelian, G., & Santos, N. C. 2010, *A&A*, 512, L5
 Sousa, S. G., Santos, N. C., Israelian, G., et al. 2011a, *A&A*, 526, A99
 Sousa, S. G., Santos, N. C., Israelian, G., Mayor, M., & Udry, S. 2011b, *A&A*, 533, A141
 Sozzetti, A., Udry, S., Zucker, S., et al. 2006, *A&A*, 449, 417
 Takeda, Y., & Kawanomoto, S. 2005, *PASJ*, 57, 45
 Takeda, Y., Honda, S., Kawanomoto, S., Ando, H., & Sakurai, T. 2010, *A&A*, 515, A93
 Tamuz, O., Ségransan, D., Udry, S., et al. 2008, *A&A*, 480, L33
 Théado, S., & Vauclair, S. 2012, *ApJ*, 744, 123
 Udry, S., & Santos, N. C. 2007, *ARA&A*, 45, 397
 Udry, S., Mayor, M., Naef, D., et al. 2000, *A&A*, 356, 590
 Xiong, D. R., & Deng, L. 2009, *MNRAS*, 395, 2013
 Zahn, J.-P. 1992, *A&A*, 265, 115
 Zhang, Q. S. 2012, *MNRAS*, 427, 1441

Table 6. Li abundances for stars without detected planets from HARPS GTO samples. Parameters from [Sousa et al. \(2008, 2011a,b\)](#)

Star	T_{eff} (K)	$\log g$ (cm s^{-2})	ξ_t (km s^{-1})	[Fe/H]	Age (Gyr)	Mass (M_{\odot})	A(Li)	Error
HARPS-1								
HD 1320	5679	4.49	0.85	-0.27	7.76	0.86	1.29	0.06
HD 2071	5719	4.47	0.95	-0.09	2.18	0.97	1.38	0.07
HD 4307	5812	4.10	1.22	-0.23	8.68	1.03	2.39	0.04
HD 4915	5658	4.52	0.90	-0.21	3.12	0.91	1.38	0.05
HD 8406	5726	4.50	0.87	-0.10	2.28	0.97	1.70	0.05
HD 11505	5752	4.38	0.99	-0.22	11.43	0.88	<0.35	-
HD 12387	5700	4.39	0.93	-0.24	11.56	0.86	<0.15	-
HD 13724	5868	4.52	1.02	0.23	0.82	1.10	1.60	0.05
HD 19467	5720	4.31	0.96	-0.14	11.74	0.91	<0.55	-
HD 20407	5866	4.50	1.09	-0.44	11.34	0.84	1.85	0.05
HD 20619	5703	4.51	0.92	-0.22	6.84	0.89	1.66	0.04
HD 20807	5866	4.52	1.04	-0.23	6.43	0.94	<0.21	-
HD 21938	5778	4.38	0.99	-0.47	11.50	0.82	1.08	0.06
HD 27063	5767	4.44	0.94	0.05	1.12	1.03	1.65	0.05
HD 28471	5745	4.37	0.95	-0.05	8.68	0.94	<0.73	-
HD 28701	5710	4.41	0.95	-0.32	11.60	0.84	<0.16	-
HD 28821	5660	4.38	0.88	-0.12	11.06	0.88	<0.11	-
HD 32724	5818	4.26	1.14	-0.17	10.88	0.96	1.58	0.05
HD 34449	5848	4.50	0.92	-0.09	0.99	1.02	2.03	0.05
HD 37962	5718	4.48	0.84	-0.20	7.86	0.89	1.79	0.05
HD 38277	5871	4.34	1.10	-0.07	8.28	1.01	1.58	0.07
HD 44420	5818	4.37	1.06	0.29	2.25	1.08	<0.71	-
HD 44594	5840	4.38	1.06	0.15	2.92	1.07	1.47	0.08
HD 45289	5717	4.32	0.99	-0.02	10.31	0.95	<0.47	-
HD 50806	5633	4.11	1.03	0.03	9.64	1.01	0.60	0.10
HD 59468	5618	4.39	0.88	0.03	8.44	0.93	<0.27	-
HD 59711A	5722	4.46	0.86	-0.12	6.81	0.92	1.22	0.10
HD 66221	5635	4.40	0.92	0.17	3.74	1.00	<0.50	-
HD 67458	5891	4.53	1.04	-0.16	3.80	0.99	2.14	0.04
HD 71334	5694	4.37	0.95	-0.09	9.19	0.91	<0.65	-
HD 72769	5640	4.35	0.98	0.30	5.86	1.00	<0.51	-
HD 76151	5788	4.48	0.96	0.12	0.90	1.05	1.82	0.05
HD 78429	5760	4.33	1.01	0.09	7.65	1.00	<0.35	-
HD 78538	5786	4.50	0.98	-0.03	1.62	1.01	2.37	0.05
HD 78558	5711	4.36	0.99	-0.44	11.73	0.92	<0.37	-
HD 78612	5834	4.27	1.14	-0.24	11.24	0.94	1.57	0.05
HD 78747	5788	4.44	1.10	-0.67	11.32	0.81	<0.94	-
HD 88084	5766	4.42	0.96	-0.10	7.76	0.93	<1.10	-
HD 88218	5878	4.16	1.23	-0.14	8.35	1.05	2.42	0.05
HD 89454	5728	4.47	0.96	0.12	1.32	1.03	1.57	0.07
HD 92719	5824	4.51	0.96	-0.10	1.06	1.01	1.90	0.04
HD 95521	5773	4.49	0.96	-0.15	2.84	0.96	1.62	0.05
HD 96423	5711	4.35	0.98	0.10	6.53	0.99	1.88	0.04
HD 97037	5883	4.34	1.13	-0.07	7.89	1.00	1.65	0.05
HD 97998	5716	4.57	0.85	-0.42	9.50	0.82	1.67	0.05
HD 104982	5692	4.44	0.91	-0.19	8.64	0.88	<0.14	-
HD 106116	5680	4.39	0.91	0.14	5.26	1.00	<0.13	-
HD 108309	5775	4.23	1.08	0.12	7.59	1.04	0.94	0.10
HD 109409	5886	4.16	1.24	0.33	4.06	1.24	2.50	0.02
HD 110619	5613	4.51	0.83	-0.41	6.33	0.82	1.11	0.10
HD 111031	5801	4.39	1.05	0.27	4.49	1.06	0.85	0.10
HD 114613	5729	3.97	1.18	0.19	4.50	1.24	2.63	0.03
HD 114853	5705	4.44	0.92	-0.23	10.51	0.87	<0.46	-
HD 115585	5711	4.27	1.14	0.35	7.48	1.04	<0.51	-
HD 115674	5649	4.48	0.85	-0.17	3.64	0.91	<0.40	-
HD 117105	5889	4.41	1.13	-0.29	11.12	0.90	1.93	0.05
HD 125184	5680	4.10	1.13	0.27	7.33	1.08	<0.39	-
HD 134664	5865	4.52	0.99	0.10	1.10	1.07	2.10	0.05
HD 140901	5610	4.46	0.90	0.09	2.31	0.98	<0.48	-
HD 143114	5775	4.39	0.92	-0.41	11.58	0.84	<0.67	-
HD 145809	5778	4.15	1.14	-0.25	9.49	1.00	2.08	0.05
HD 146233	5818	4.45	1.00	0.04	2.22	1.03	1.57	0.07
HD 154962	5827	4.17	1.22	0.32	4.67	1.20	2.31	0.02
HD 157347	5676	4.38	0.91	0.02	8.22	0.94	<0.38	-

Table 6. continued.

Star	T_{eff} (K)	$\log g$ (cm s^{-2})	ξ_t (km s^{-1})	[Fe/H]	Age (Gyr)	Mass (M_{\odot})	A(Li)	Error
HD 161612	5616	4.45	0.88	0.16	2.05	1.00	<0.45	–
HD 171665	5655	4.41	0.89	–0.05	4.72	0.94	1.64	0.05
HD 177409	5898	4.49	0.99	–0.04	1.01	1.05	2.31	0.05
HD 177565	5627	4.39	0.91	0.08	5.60	0.96	<0.49	–
HD 177758	5862	4.41	1.11	–0.58	11.74	0.90	1.68	0.10
HD 183658	5803	4.40	1.00	0.03	5.97	1.00	1.09	0.10
HD 188748	5623	4.43	0.83	–0.12	3.27	0.92	<0.33	–
HD 189625	5846	4.43	1.03	0.18	1.08	1.09	2.06	0.06
HD 190248	5604	4.26	0.99	0.33	8.74	0.98	<0.59	–
HD 195564	5676	4.03	1.11	0.06	7.51	1.08	1.97	0.05
HD 198075	5846	4.56	0.95	–0.24	2.01	0.96	1.95	0.07
HD 202605	5658	4.49	1.02	0.18	2.73	1.01	1.19	0.10
HD 203432	5645	4.39	0.98	0.29	5.81	1.00	<0.45	–
HD 206172	5608	4.49	0.77	–0.24	2.94	0.89	1.27	0.10
HD 207700	5666	4.29	0.98	0.04	10.85	0.96	<0.42	–
HD 208704	5826	4.38	1.04	–0.09	9.01	0.95	1.09	0.10
HD 210918	5755	4.35	0.99	–0.09	10.80	0.93	<0.28	–
HD 211415	5850	4.39	0.99	–0.21	9.44	0.92	1.80	0.05
HD 212708	5681	4.35	0.99	0.27	4.77	1.02	<0.55	–
HD 213575	5671	4.18	1.02	–0.15	11.65	0.95	<0.38	–
HD 214385	5654	4.43	0.81	–0.34	10.64	0.82	<–0.30	–
HD 216777	5623	4.51	0.81	–0.38	7.02	0.82	1.63	0.05
HD 220507	5698	4.29	1.01	0.01	10.62	0.96	<0.56	–
HD 221146	5876	4.27	1.09	0.08	6.43	1.09	<0.98	–
HD 221420	5847	4.03	1.28	0.33	3.76	1.29	2.65	0.02
HD 222595	5648	4.46	0.88	0.01	1.19	0.98	<0.58	–
HD 222669	5894	4.46	1.01	0.05	1.12	1.07	2.00	0.03
HD 223171	5841	4.20	1.12	0.12	6.33	1.10	2.05	0.03
HD 224393	5774	4.54	0.84	–0.38	3.73	0.87	2.21	0.04
HARPS-4								
HD 16784	5837	4.34	1.14	–0.65	11.35	0.86	1.52	0.12
HD 17865	5877	4.32	1.16	–0.57	11.47	0.89	1.77	0.04
HD 22879	5884	4.52	1.20	–0.81	11.38	0.81	1.63	0.05
HD 51754	5848	4.49	1.05	–0.55	8.16	0.85	1.12	0.10
HD 56274	5734	4.51	0.94	–0.54	6.15	0.83	2.11	0.03
HD 69611	5762	4.31	0.99	–0.58	11.31	0.85	<0.89	–
HD 75745	5885	4.29	1.34	–0.78	0.00	0.00	2.42	0.04
HD 77110	5717	4.48	0.86	–0.50	7.90	0.84	1.18	0.08
HD 79601	5825	4.32	1.09	–0.59	11.43	0.85	1.22	0.06
HD 88725	5654	4.49	0.86	–0.64	10.71	0.80	<0.02	–
HD 97783	5682	4.50	0.88	–0.73	7.75	0.79	<0.15	–
HD 104800	5697	4.47	0.87	–0.79	6.34	0.78	<0.65	–
HD 105004	5756	4.33	0.80	–0.81	4.30	0.79	1.86	0.05
HD 111777	5666	4.46	0.82	–0.68	8.48	0.79	<0.44	–
HD 113679	5768	4.26	1.08	–0.61	6.37	0.83	2.11	0.05
HD 121004	5687	4.48	0.76	–0.71	6.31	0.79	<0.64	–
HD 124785	5867	4.20	1.29	–0.56	7.66	1.02	<0.98	–
HD 129229	5872	3.89	1.37	–0.42	5.04	1.13	<0.32	–
HD 134088	5675	4.46	0.86	–0.75	9.75	0.78	1.10	0.12
HD 134113	5782	4.25	1.27	–0.74	10.92	0.88	1.90	0.05
HD 147518	5626	4.40	0.67	–0.63	6.34	0.80	<0.54	–
HD 149747	5823	3.95	1.28	–0.34	0.00	0.00	<1.48	–
HD 167300	5837	4.30	1.05	–0.45	10.15	0.94	1.69	0.07
HD 175179	5764	4.46	0.88	–0.66	6.93	0.81	<0.53	–
HD 193901	5611	4.41	0.54	–1.07	7.64	0.74	1.90	0.05
HD 197083	5735	4.50	0.90	–0.45	6.62	0.85	1.38	0.06
HD 197197	5812	4.20	1.25	–0.46	10.98	0.93	2.11	0.03
HD 199288	5746	4.46	0.93	–0.63	11.41	0.82	0.94	0.10
HD 199604	5817	4.34	1.04	–0.62	10.63	0.83	1.46	0.10
HD 199847	5763	4.22	1.04	–0.54	9.61	0.85	1.28	0.12
HD 206998	5822	4.24	1.13	–0.69	10.80	0.89	2.04	0.05
HD 224817	5894	4.36	1.13	–0.53	11.08	0.91	1.80	0.04
BD +083095	5728	4.12	0.85	–0.77	0.00	0.00	2.00	0.08
HARPS-2								
HD 67	5746.	4.56	1.02	0.03	1.73	0.98	1.91	0.05

Table 6. continued.

Star	T_{eff} (K)	$\log g$ (cm s^{-2})	ξ_t (km s^{-1})	[Fe/H]	Age (Gyr)	Mass (M_{\odot})	A(Li)	Error
HD 1979	5626.	4.52	0.74	-0.09	4.65	0.92	<0.80	-
HD 3220	5846.	4.51	0.87	-0.22	3.02	0.94	2.24	0.05
HD 3964	5729.	4.50	0.85	0.05	3.09	0.99	<1.31	-
HD 4021	5831.	4.71	1.32	0.02	1.88	1.00	2.48	0.10
HD 8038	5694.	4.45	0.88	0.15	3.52	1.01	<1.20	-
HD 8930	5687.	4.52	0.79	-0.23	4.27	0.90	1.75	0.10
HD 10895	5685.	4.52	0.78	-0.27	5.06	0.88	1.72	0.08
HD 13578	5842.	4.18	1.12	-0.03	7.59	1.04	2.11	0.04
HD 14868	5864.	4.44	0.90	0.02	1.87	1.02	1.71	0.10
HD 16008	5712.	4.42	0.78	-0.09	5.72	0.94	1.62	0.10
HD 16548	5690.	3.96	1.15	0.15	5.25	1.19	2.44	0.04
HD 17439	5721.	4.44	0.87	0.08	3.05	1.00	<0.42	-
HD 18001	5772.	4.44	0.80	-0.07	3.05	0.96	1.28	0.10
HD 19423	5752.	4.23	0.96	-0.09	10.10	0.96	<0.20	-
HD 19641	5806.	4.39	0.94	-0.01	4.60	0.99	1.37	0.10
HD 22177	5666.	4.26	1.02	0.20	8.05	1.03	<0.38	-
HD 22249	5773.	4.63	0.96	-0.06	2.57	0.96	2.48	0.08
HD 25912	5900.	4.52	0.99	0.12	1.37	1.06	2.15	0.05
HD 26729	5718.	4.17	1.13	0.31	6.00	1.13	1.70	0.07
HD 27471	5871.	4.25	1.13	0.11	5.31	1.14	2.18	0.05
HD 29137	5768.	4.28	1.10	0.30	6.29	1.08	<0.84	-
HD 29263	5780.	4.35	0.94	0.03	7.02	1.00	<0.76	-
HD 29303	5819.	4.52	0.93	-0.12	3.24	0.97	2.23	0.08
HD 29428	5743.	4.48	0.82	-0.06	2.59	0.95	1.78	0.10
HD 31532	5896.	4.07	1.33	-0.08	4.55	1.22	1.92	0.07
HD 33822	5726.	4.29	0.98	0.26	6.79	1.05	<1.41	-
HD 34327	5883.	4.20	1.19	-0.06	6.51	1.11	2.46	0.06
HD 38078	5651.	4.47	0.62	-0.29	5.42	0.87	<1.31	-
HD 39427	5682.	4.52	0.86	-0.18	4.24	0.91	1.61	0.07
HD 40865	5722.	4.49	0.91	-0.38	6.68	0.86	1.10	0.10
HD 41248	5713.	4.49	0.84	-0.37	4.99	0.86	1.56	0.10
HD 41323	5756.	4.56	0.84	-0.31	4.20	0.89	1.81	0.06
HD 48115	5825.	4.48	0.89	-0.19	3.23	0.95	2.17	0.05
HD 49035	5640.	4.35	1.01	0.24	4.07	1.00	<0.51	-
HD 61383	5716.	4.20	1.12	-0.49	11.41	0.92	2.04	0.05
HD 61447	5637.	4.37	0.89	0.17	3.75	0.99	<0.89	-
HD 61986	5725.	4.48	0.85	-0.34	5.81	0.87	1.18	0.12
HD 62128	5828.	4.22	1.16	0.33	5.26	1.12	<0.83	-
HD 72374	5767.	4.35	0.90	-0.09	7.77	0.95	<0.75	-
HD 74698	5783.	4.27	1.01	0.07	7.49	1.02	<0.64	-
HD 76440	5764.	4.43	0.89	-0.01	3.71	0.98	<0.59	-
HD 81700	5882.	4.53	0.98	0.12	1.52	1.06	2.18	0.05
HD 87320	5639.	4.41	0.95	-0.17	9.27	0.90	<0.88	-
HD 90702	5760.	4.56	1.04	0.20	1.96	1.04	1.92	0.08
HD 90722	5711.	4.28	1.06	0.31	6.58	1.03	<0.37	-
HD 91345	5658.	4.52	0.72	-1.04	8.73	0.75	1.61	0.10
HD 94771	5631.	4.03	1.10	0.22	6.83	1.11	1.52	0.08
HD 96116	5832.	4.52	0.96	-0.01	2.74	1.00	2.12	0.07
HD 101339	5731.	4.48	0.88	-0.10	4.26	0.95	1.21	0.10
HD 101367	5615.	4.38	0.91	0.29	7.30	0.99	<0.82	-
HD 101644	5678.	4.58	0.72	-0.56	5.04	0.82	2.05	0.05
HD 105779	5792.	4.51	0.91	-0.25	4.05	0.92	1.63	0.08
HD 108768	5633.	4.45	0.86	0.14	2.80	0.98	<0.79	-
HD 109098	5888.	4.14	1.24	0.06	5.42	1.14	2.48	0.05
HD 109723	5647.	4.47	0.88	-0.04	3.18	0.93	1.58	0.20
HD 110668	5850.	4.45	0.98	0.17	2.22	1.07	1.60	0.15
HD 113513	5751.	4.54	0.94	0.17	1.49	1.01	1.88	0.20
HD 114561	5829.	4.50	0.88	-0.07	2.97	0.99	<1.10	-
HD 115902	5705.	4.39	0.86	-0.01	4.36	0.96	<0.74	-
HD 116259	5700.	4.21	0.99	0.11	8.56	1.02	<0.45	-
HD 119173	5779.	4.26	0.52	-0.62	5.66	0.82	1.94	0.10
HD 120344	5623.	4.42	0.65	-0.19	5.24	0.90	<0.42	-
HD 122474	5716.	4.37	0.88	0.13	3.48	1.01	<0.77	-
HD 123319	5619.	4.56	0.67	-0.52	4.45	0.81	2.31	0.03
HD 129191	5832.	4.39	0.99	0.24	2.49	1.08	1.12	0.10

Table 6. continued.

Star	T_{eff} (K)	$\log g$ (cm s^{-2})	ξ_t (km s^{-1})	[Fe/H]	Age (Gyr)	Mass (M_{\odot})	A(Li)	Error
HD 131183	5670.	4.24	0.97	0.09	9.36	0.99	<0.33	–
HD 131218	5797.	4.55	0.96	–0.06	2.48	0.97	2.18	0.07
HD 131565	5612.	4.47	0.72	–0.16	5.84	0.90	<1.23	–
HD 134702	5782.	4.50	0.74	–0.04	3.20	0.98	1.98	0.08
HD 140785	5756.	4.12	1.09	–0.05	7.28	1.09	2.08	0.05
HD 141624	5871.	4.40	1.01	–0.38	8.59	0.88	1.61	0.15
HD 142879	5707.	4.51	0.74	–0.39	5.03	0.85	1.84	0.08
HD 145927	5819.	4.41	0.93	–0.03	2.74	0.99	<0.46	–
HD 148577	5713.	4.29	0.95	–0.09	10.46	0.96	<0.16	–
HD 149396	5657.	4.47	0.91	0.19	4.95	1.00	<0.71	–
HD 149724	5747.	4.24	1.08	0.37	6.57	1.07	2.08	0.06
HD 150437	5826.	4.29	1.09	0.30	4.63	1.08	1.46	0.15
HD 151933	5849.	4.29	1.03	–0.21	5.32	0.94	1.61	0.07
HD 155968	5790.	4.42	0.92	0.16	2.46	1.04	<0.90	–
HD 156079	5892.	4.24	1.16	0.28	4.29	1.21	2.27	0.04
HD 161256	5652.	4.27	0.93	0.14	6.97	0.99	<0.18	–
HD 161555	5850.	4.15	1.23	0.12	5.14	1.16	2.64	0.06
HD 165131	5870.	4.45	0.99	0.06	2.43	1.04	1.53	0.10
HD 166745	5621.	4.31	0.98	0.25	5.06	1.00	<0.15	–
HD 171942	5615.	4.42	0.72	–0.10	4.54	0.92	<–0.33	–
HD 172568	5728.	4.58	0.78	–0.37	5.48	0.86	<0.38	–
HD 172643	5645.	4.50	0.73	–0.15	3.51	0.90	1.29	0.20
HD 178904	5727.	4.41	0.98	0.09	6.10	1.00	<0.52	–
HD 186302	5662.	4.44	0.78	–0.03	3.63	0.95	<–0.29	–
HD 190524	5825.	4.50	0.85	–0.13	4.21	0.96	2.10	0.07
HD 190613	5776.	4.33	0.95	0.00	7.14	0.98	1.31	0.15
HD 195145	5625.	4.41	0.82	0.17	3.61	0.99	<0.28	–
HD 200633	5853.	4.51	1.01	0.05	2.41	1.03	<1.27	–
HD 201422	5841.	4.63	0.98	–0.16	2.82	0.96	2.45	0.07
HD 204287	5743.	4.15	1.10	–0.04	8.73	1.03	1.52	0.05
HD 209449	5854.	4.16	1.19	0.41	4.69	1.18	2.32	0.05
HD 210272	5713.	4.13	1.16	–0.22	8.53	1.04	2.02	0.05
HD 212036	5687.	4.41	0.80	–0.01	5.05	0.96	<0.04	–
HD 212231	5762.	4.20	1.01	–0.30	11.06	0.92	<1.00	–
HD 214867	5807.	4.66	1.23	0.01	1.82	0.99	2.41	0.08
HD 214954	5738.	4.48	0.99	0.14	4.83	1.02	<0.77	–
HD 216008	5773.	4.38	0.91	–0.04	6.13	0.97	<0.52	–
HD 218340	5889.	4.42	0.97	0.09	2.05	1.06	2.07	0.05
HD 218885	5763.	4.46	0.80	–0.28	3.26	0.89	2.01	0.10
HD 220456	5887.	4.50	1.01	–0.02	2.00	1.02	2.26	0.05
HD 221343	5848.	4.54	0.99	0.11	1.56	1.04	1.95	0.07
HD 223315	5650.	4.44	0.89	0.30	1.79	1.00	<1.03	–
HIP 99606B	5764.	4.19	0.98	–0.41	3.55	0.86	1.68	0.10